The Pennsylvania State University

The Graduate School

Department or Civil and Environmental Engineering

THE EFFECTS OF FLUID'S PHYSICOCHEMICAL CHARACTERISTICS ON PIPING EROSION PROGRESSION OF A SILTY SAND

A Thesis in

Civil Engineering

by

Yuetan Ma

Submitted in Partial Fulfillment
of the Requirements
for the Degree of

Master of Science

May 2018

The thesis of Yuetan Ma was reviewed and approved* by the following:

Ming Xiao
Associate Professor of Civil Engineering
Thesis Advisor

Xiaofeng Liu
Assistant Professor of Civil Engineering

Sai P. Kakuturu
Associate Professor of Civil Engineering

Patrick J. Fox
Department Head of Civil and Environmental Engineering

*Signatures are on file in the Graduate School

ABSTRACT

This thesis presents an experimental research for studying the absolute and interactive effects of three physicochemical characteristics of permeating fluids (viscosity, pH, and ionic strength) on piping erosion progression of a sandy soil under turbulent flow. Full factorial experimental design was used to produce eight types of fluids of various combinations of the three fluid characteristics. Hole erosion tests were conducted on identically prepared silty clayey sand specimens. Erosion rate index, an important index was used to quantify the relative erosive capacity of the test fluids. The erosion rate index was quantified for two repeat trials for each of the eight test fluids. Regression analysis was conducted on the results to generate a statistic model to describe the effects of the three factors and their interactions. The main findings include: (1) Viscosity, pH and ionic strength were all determined to be significant factors on the rate of erosion. The two-way interactions between viscosity and pH, and between viscosity and ionic strength were also determined to be significant interaction factors, while the interaction between pH and ionic strength did not prove to be statistically significant. (2) Higher pH causes higher erosive capacity; higher ionic strength causes lower erosive capacity of fluid. (3) At low viscosity, ionic strength does not affect the erosion; but when the viscosity is higher (or the fluid temperature is colder), higher ionic strength causes much less erosion. There is almost no interactive effect between pH and ionic strength.

TABLE OF CONTENTS

LIST OF FIGURES

LIST OF TABLES

ACKNOWLEDGEMENTS

First, I would like to thank my advisor Dr. Ming Xiao for his encouragement and guidance during my graduate study. I am honored to work with him. And I would like to express my gratitude to my thesis committee members Dr. Xiaofeng Liu and Dr. Sai P. Kakuturu for their advice and input in the development of the thesis.

Second, I wish to show my appreciation to my research group, particularly Behnoud Kermani and Jintai Wang. I want to thank Behnoud for helping me do the HET tests and thank Jintai for giving me some useful advice. Research is like a journey, because of their encouragement and assistance, I have succeeded to keep on enjoying it.

Finally, I would like to sincerely thank my father Jiankun Ma and my mother Liping Wang for their support throughout my educational endeavor.

CHAPTER 1 INTRODUCTION

1.1 Background

1.1.1 Piping and Backward Erosion

Dams are considered as "installations containing dangerous forces" under International Humanitarian Law due to the massive impact of a possible destruction on the civilian population and the environment (Baker, 1991). Dam failures are comparatively rare but can cause immense damage and loss of life when they occur. Piping is known to cause catastrophic failures of levees and earthen dams (Seed et al., 2008; Terzaghi, 1943) and has been studied for many years. In the recent years, several disasters in bridge foundations, quarries, levees and earthen dams indicate that soil erosion is a main factor of failure. (Fry et al., 1997; Guiton, 1998; Foser et al., 2000; Fell and Fry, 2007; Briaud, 2008). Two types of erosion can be distinguished: surface erosion that occurs at the soil and water interface and internal (subsurface) erosion, which takes place inside the soil matrix.

Several authors have concluded that soil structures can be divided into two groups: A primary structure and a secondary structure (Barakat, 1991; Kenney and Lau, 1986; Lafleur et al., 1989; Tomlinson and Vaid, 2000). Basically, the primary structure is a network of grains that form the skeleton of the soil matrix, while the secondary structure is the fines that are in the voids of the primary structure. In internal erosion, there exist two types: one is piping and backwards erosion, which affects both the primary and secondary structures. The other is suffusion that primarily affects only the secondary soil structures.

The piping progression process includes piping mobilization, particle transport, and particle deposition. Soil particles are removed from a soil matrix (i.e., dislodging) when the hydraulic shear forces exerted by seepage flow exceed the forces that keep the particles within the soil matrix. The dislodging of these particles can gradually form a continuous, tubular cavity that resembles a pipe.

Backward erosion is an internal erosion mechanism, during which shallow pipes are formed in the direction opposite to the flow underneath water-retaining structures as a result of the gradual removed soil by the action of water. It is an important failure mechanism in both dikes and dams where sandy layers are covered by a cohesive layer; it occurs rapidly leaving little time for reaction (Charles, 1997). Figure 1-1 illustrates the progression of piping and backward erosion.

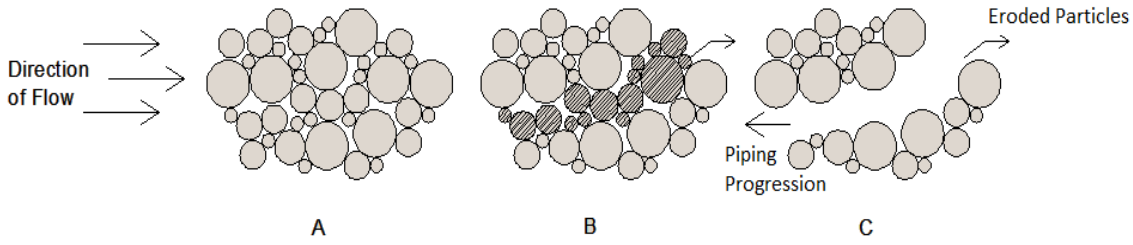

Figure 1-1. Progression of piping and backward erosion (Shwiyhat, 2010)

Piping and backward erosion are detected at the landside face of a levee or earthen dam. Wet spots, sand boils, and sand heaves are used as the indicators of such activities. Wet spots are areas on the land side of a levee or earthen dam that has become saturated due to seepage. Sand boils and heaves occur when it reaches to the critical hydraulic

gradient, which pushes against the downward vertical force of soil until an exit point is created. Figure 1-2 shows a photo of sand boil.

Figure 1-2. Sand bags placed around a sand boil (Hickman, KY, 2011)

1.1.2 Suffusion

Suffusion is defined as the detachment and migration of fine grained particles through the pores of a soil matrix that is composed of coarse grained particles (Bendahmane et al., 2008). The detachment and migration of coarse grained particles are the result of seepage flow through a hydraulic structure. This type of internal erosion affects the secondary structure of a soil matrix and can increase the potential differential settlement and permeability of the soil. But suffusion is a long-time process that can take up to several years. As for the micro structures in suffusion, grains of the secondary structure are entrained into seepage flow and eroded out from the spaces between large particles. As time goes, the primary structures finally remain in contact and static. The diameter of the

fine grains that are removed must be smaller than that of the pore throat, or pore clogging will occur. Figure 1-3 illustrates the progression of suffusion.

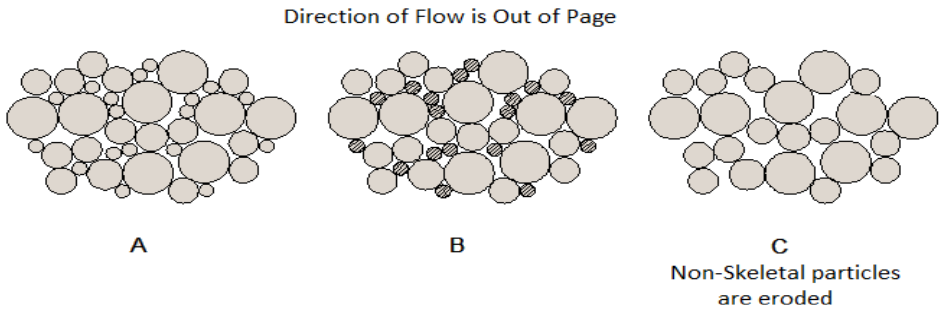

Figure 1-3. Progression of suffusion (Shwiyhat, 2010)

The characteristics of soil greatly contribute to the process of suffusion. This erosion is typical of a gap graded or segregated material. So, careful selection of materials can in most cases help alleviate the problems that lead to suffusion.

1.1.3 Remediation of Internal Erosion

Figure 1-4 shows a slurry cut-off wall, which is an impermeable barrier that is installed in an earthen embankment and penetrates the underlying permeable foundation soil. It is considered the most effective means of eliminating seepage and subsurface erosion problems and is widely used. Cut-off walls include slurry walls and sheet pile walls. A slurry wall is installed by first excavating a trench that is backfilled with slurry. There are various types of slurry materials, such as cement-bentonite slurry, soil-cement-bentonite slurry, and soil-bentonite slurry. The slurry solidifies into an impermeable wall along the longitudinal direction of the levee or earthen dam. A sheet pile wall is made of interlocking steel sheet piles that are driven through the embankment and into the foundation soil using a vibratory hammer. A cut-off wall should penetrate most (such as

95%) of the permeable soil stratum. If the pervious foundation soil has significant depth, installing cut-off walls may not be economical.

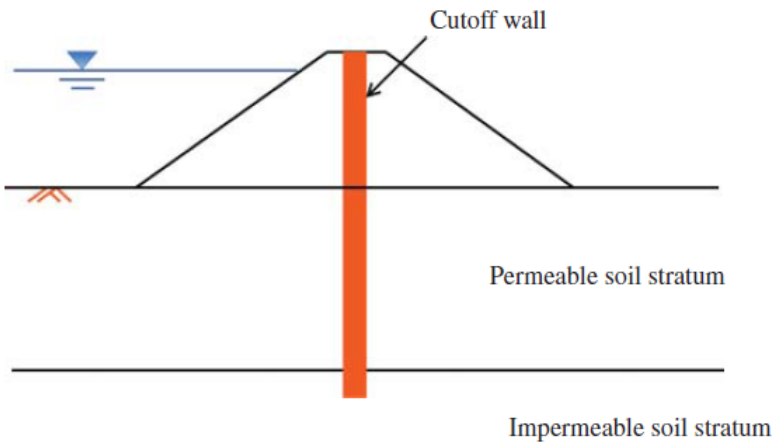

Figure 1-4. Cross-section view of a slurry cut-off wall in a levee (After USACE, 2000)

1.2 Research Motivation and Objectives

In the case of water-retaining embankments such as dams and levees, which are essential for the safety and quality of life for people throughout the world, subsurface erosion (internal erosion) is of particular concern and many catastrophic failures have been attributed to its potentially destructive consequences, including the 1972 failure of the Buffalo Creak Dam in West Virginia (Davies et al., 1972), the 1976 Teton Dam failure in Idaho (Penman, 1987; Sherard, 1987), the 1990 Cyanide Dam failure in North Carolina (Leonards and Deschamps, 1998), and three levee breaches during Hurricane Katrina in 2005 (Seed et al., 2008a; Sills et al., 2008b).

In previous experimental studies on internal erosion, tap water or de-ionized water have often been used as a permeating fluid. However, when the fluid permeates through

soil and interacts with the environment, its properties are altered from those of pure water (Hillel, 1998). Significant research has been conducted in the past to investigate the effects of physicochemical characteristics of fluids (with focus on pH and ionic strength) on the incipient motions of colloidal-size (<1 μm) particles, such as glass microspheres (Sharma et al. 1992) and colloidal titanium hydrous oxide spheres (Hubbe, 1985). These studies generally concluded that higher pH and lower ionic strength result in easier particle mobilization. Limited research has been conducted on the effects of permeating fluid's physicochemical characteristics on soil's erosion behaviors. Past research preliminarily revealed the individual effects of a fluid's viscosity, pH, and ionic strength on the mobilization of colloidal particles and the erosion of clayey soils. Whether and how these physicochemical characteristics affect the piping progression on sandy soil is unknown. Therefore, the main objective of this research is to reveal the relative and interactive of fluid's physicochemical characteristics (viscosity, pH and ionic strength) on piping erosion progression of a sandy soil.

1.3 Methodology

The erosion characteristics are often described by the erosion rate index and critical shear stress. Critical shear stress is the minimum hydraulic shear stress required to mobilize a particle, also known as incipient motion. Piping erosion progression is often indicated by erosion rate index, which is quantified in this research for fluids with various combinations of physicochemical characteristics. In this research, three physicochemical characteristics (factors) of fluid were studied: pH, ionic strength, and viscosity. Distilled water was used

as the base of each test fluid. Each fluid parameter had a target low and high levels. The experimental design approach followed three-factor, two-level, full factorial design. Hole erosion test (HET) was used to simulate piping erosion process and the method given by Wan and Fell (2004) was used to calculate the erosion rate index of each permeating fluid. Regression analysis, ANOVA (analysis of variance), was used to show the relative and interactive effects of viscosity, pH and ionic strength on piping progression of a sandy soil.

1.4 Organization

This thesis consists of five chapters. Following the introduction in this chapter, Chapter 2 presents a synthesis of published studies on erosion testing, particle fate in porous media, and internal erosion influenced by permeating fluids.

Chapter 3 presents the research materials and methodology, including the experimental setup of HET tests, fluids preparation, direct shear testing of soils in different temperatures, HET data processing, regression analysis of HET results and determination of shear strength under different temperatures.

Chapter 4 presents the results and analysis, including the results of erosion rate index calculations and the results of regression analysis.

Chapter 5 presents the conclusions from this research.

CHAPTER 2 LITERATURE REVIEW

Many researchers have dedicated their work to studying the process of internal erosion. This chapter provides a review of literature that is relevant to this topic, which includes a review of erosion testing, a review of particle's fate in porous media and internal erosion affected by different permeating fluids.

2.1 Review of Erosion Testing

Many tests are designed to measure the erodibility of soil, such as dispersivity test, surface erosion tests, and internal erosion tests. Dispersivity tests include the pinhole test, Emerson crumb test, and double hydrometer test. Flume test, jet erosion test (JET), and rotating cylinder test are utilized in testing the surface erosion. As for the internal erosion, there exist two typical tests: the slot erosion test (SET) and the hole erosion test (HET).

2.1.1 Dispersivity Test

The pinhole test (Sherard et al., 1976) was designed to measure the dispersivity and erodibility of the soil (ASTM-D-4647). The schematic of the pinhole test apparatus is shown in Figure 2-1. The dimensions of the specimen are 38-mm in length and 25-mm in diameter. A 1-mm hole is punched through the center of the specimen with an awl. Distilled water from the constant head tank can pass the specimen at different head gradients. The

graduated cylinder is used to collect the effluent material and then measure the turbidity of the soil. At the end of the test, the size and shape of the hole are recorded.

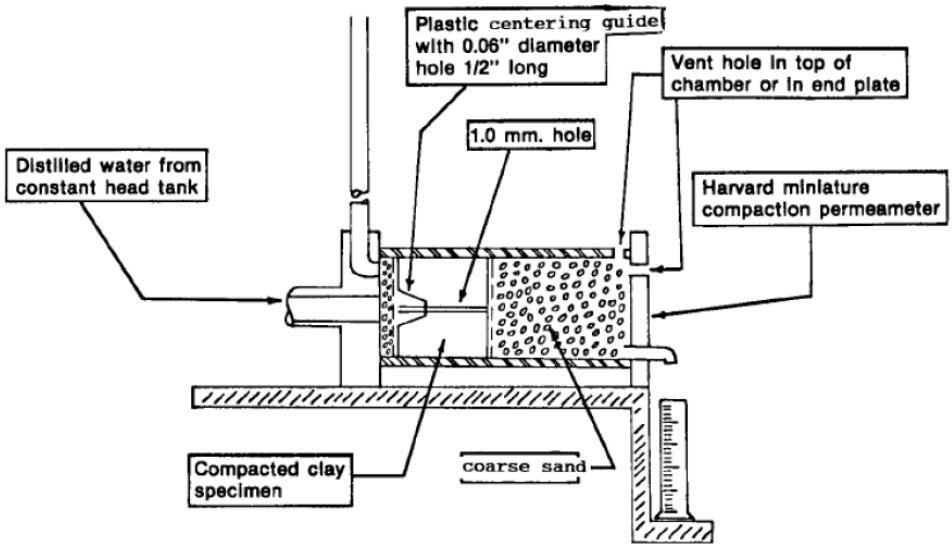

Figure 2-1. A schematic of pinhole test apparatus (ASTM, 2006)

The crumb test (Emerson, 1964) contained a cube of remolded soil with approximately 15-mm. The temperature of the water was recorded, and visual determinations of the dispersion grade were recorded at 2 min, 1 h, and 6 h. Determination of grade was based on the formation, extent and turbidity of a dense “cloud” extending from the soil crumb. Determinations can be divided into four levels: Grade 1 (Non-Dispersive), Grade 2 (Intermediate), Grade 3 (Dispersive), and Grade 4 (Highly Dispersive).

As for the double hydrometer test, 50-grams of oven dried soils were placed in 125-mL of distilled water for up to two hours. Then the soil mixture was placed in the sedimentation cylinder with the water added until the total volume reached 1000 mL. After

the time was recorded, the hydrometer temperature reading was taken to determine the percentage of material finer than 5 μm in suspension. At last, the percent dispersion was calculated using equation (1).

$$\%\ \text{Dispersion} = \frac{\%\ \text{passing}\ 5-\mu m\ \text{in the test}}{\%\ \text{passing}\ 5-\ \mu m\ \text{in Test Method D442}} \times 100 \quad (1)$$

2.1.2 Surface Erosion Test

Briefly speaking, the flume test (Gibbs, 1962; Kandiah and Arulanandan, 1974; Arulanandan and Perry, 1983) was aimed to measure erosion of soils in channels. Jet erosion test was designed to study the surface of the soil under an imposed constant water flow using one fixed jet or several mobile water jets (Moore and Masch, 1962; Hanson, 1991; Hanson and Robinson, 1993). Rotating cylinder test (Moore and Masch, 1962; Arulanandan et al., 1973; Kandiah and Arulanandan, 1974; Sqrgunan, 1977; Arulanandan and Perry, 1983; Chapuis, 1986) determined the critical shear stress and erosion rate, which was used to study the relationship between erosion characteristics and soil properties.

2.1.3 Internal Erosion Test

The slot erosion test (SET) and hole erosion test (HET) (Wan and Fell, 2002) were designed to study the erosion rate and the critical hydraulic shear stress required in initiating piping erosion in earthen hydraulic structures. Figure 2-3 shows a schematic diagram of the SET test apparatus. A 2.2 mm wide × 10 mm deep × 1 m long slot is formed along one surface of soil sample and the erosion of the slot can be observed during the test. An eroding fluid is passing through the slot in the soil sample box to initiate the erosion. The width of the preformed slot is measured at chosen time intervals as it is widened by erosion.

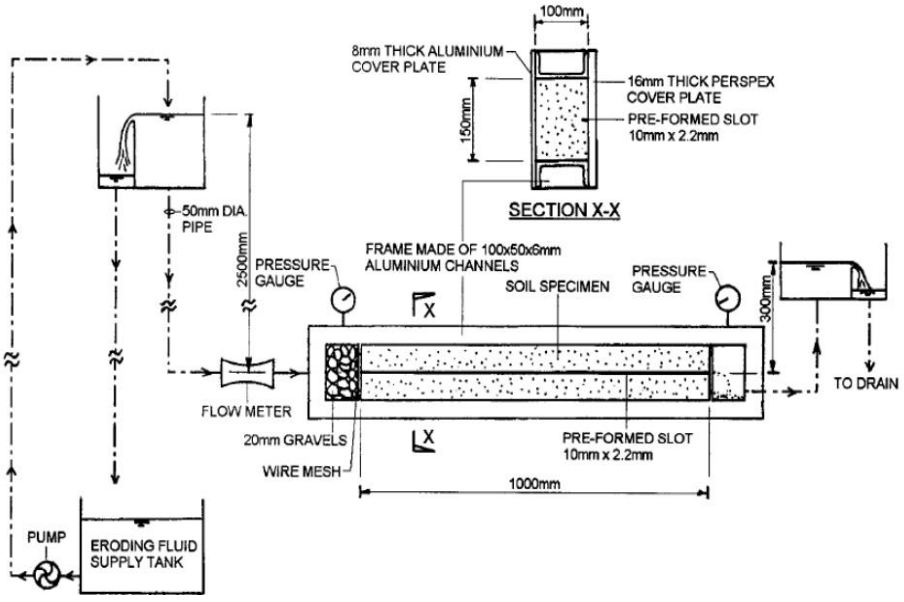

Figure 2-2. Schematic of slot erosion test (Wan and Fell, 2002)

Figure 2-3 shows a schematic of the hole erosion test (HET), which is smaller scale but the similar principle compared to SET test. Soil can be easily compacted into a standard compaction mold. After compaction, a 6 mm-diameter hole is drilled through the center of the soil specimen to simulate a pre-existing piping channel. The downstream of HET is set as 100 mm and it is necessary to conduct some trial test to choose an appropriate upstream constant head for each soil sample. Basically, the upstream water head is set at about 50 to 1200 mm higher than the downstream water head. Flow rate is used to measure the diameter of the hole indirectly.

The methods of calculating flow rate and hydraulic shear stress for both HET and SET test are almost the same. Past erosion tests have shown an approximately linear relationship between the erosion rate and the hydraulic shear stress. The equation can be expressed as:

$$\dot{\varepsilon}_t = C_e(\tau_t - \tau_c) \quad (2)$$

where $\dot{\varepsilon}_t$ = rate of erosion per unit surface area of the slot/ hole at time t (kg/s/ m^2) ; C_e = coefficient of soil erosion (s/m); τ_t = the hydraulic shear stress along the slot/hole at time t $\left(N/m^2\right)$, and τ_c = the critical shear stress $\left(N/m^2\right)$

C_e obtained from the various HET or SET tests is a small number with the range from 10^{-1} to 10^{-6}. The author of the thesis found it convenient to use the erosion rate index I_e (with a range of 0 to 6) to get the plotting results. The equation of I_e can be expressed as:

$$I_e = -\log C_e \quad (3)$$

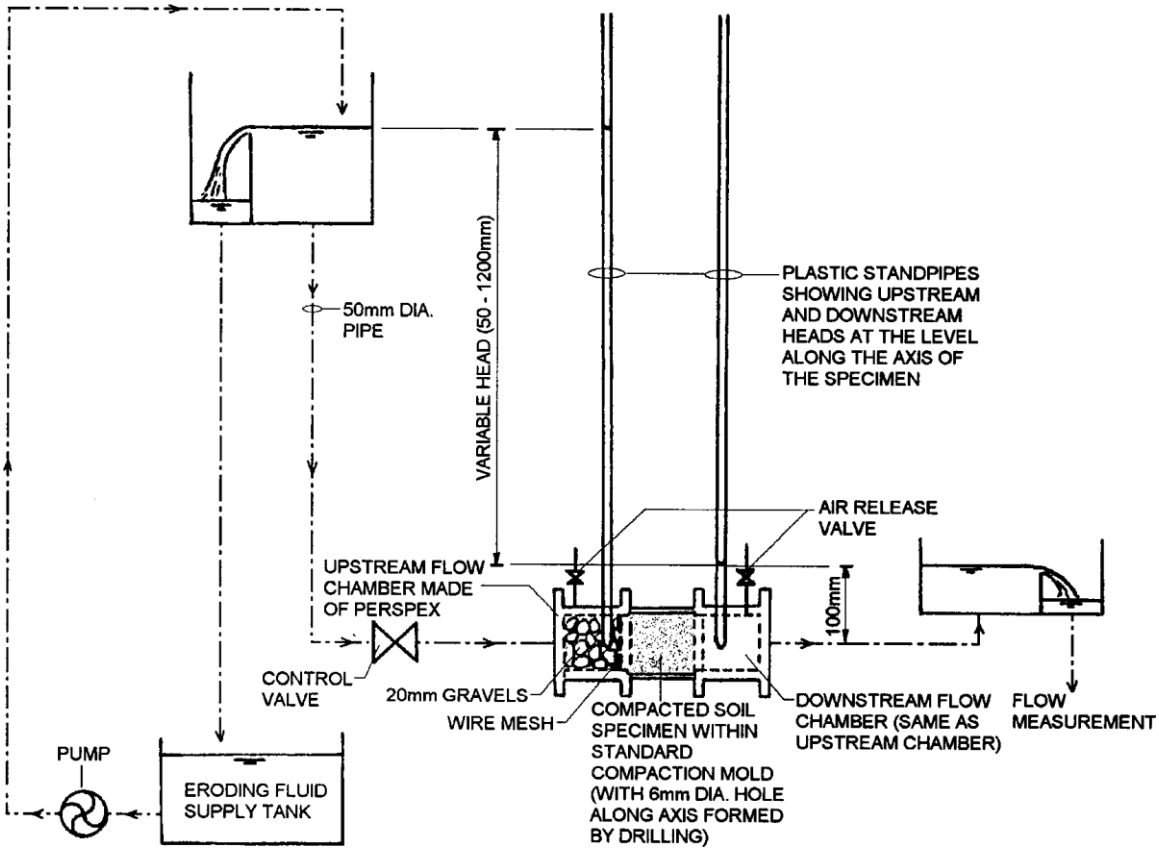

Figure 2-3. Schematic of hole erosion test (Wan and Fell, 2002)

According to the Equation (3), I_e has the inverse relationship with C_e, which means that the higher the erosion rate index, the lower the erosion.

Predicting formulas of the erosion rate index obtained by HET and SET were also proposed by Wan and Fell (2002, 2003). With adjusted R^2 values 0.77 and 0.73, the predictions were based on statistical analysis of 59 sets of coarse grain and 98 sets of fine grain test data. The predictive equation for coarse grain soil is:

$$\hat{I}_{HET-c} = 6.62 - 0.016\rho_d - 0.10\frac{\rho_d}{\rho_{max}} - 0.044\omega - 0.074\Delta\omega_r + 0.11S + 0.061Clay \quad (4)$$

where $\hat{I}_{HET-c}$ = the prediction erosion rate index for coarse grained soils; ρ_d = the dry density of the soil in Mg/m^3; ρ_d/ρ_{max} = the percent compaction (by standard proctor); ω = the water content in percent; $\Delta\omega_r$ = the water content ratio defined as $100\% \times (\omega - \omega_{opt}/\omega_{opt})$; where ω_{opt} = the optimum water content; *S* = the degree of saturation; and *Clay* = the percent clay by Unified Soil Classification (<5 μm).

The Atterberg limits and Pinhole results are incorporated into the predictive equations for fine grain soils as follows:

$$\hat{I}_{HET-f} = -10.2 + 9.57\rho_d - 0.042\frac{\rho_d}{\rho_{max}} + 0.1\omega + 0.0097\Delta\omega_r - 0.0056Fines + 0.042Clay - 0.09LL + 0.11I_p + 0.44Pinhole \quad (5)$$

where $\hat{I}_{HET-f}$ = the prediction erosion rate index for fine grained soils; *Fines* = the percent fines by United Soil Classification (<75μm); *LL* = the liquid limit in percent; I_p = the plastic index in percent, and *Pinhole* = the pinhole test classification expressed as number (i.e. 1 for class D1, 2 for class D2, etc.)

2.2 Review of Particle's Fate in Porous Media

The particle's fate is considered to occur in three processes: particle mobilization, particle transport, and particle deposition.

2.2.1 Particle Mobilization

Particle mobilization is a fundamental aspect in the process of soil erosion and involves the balance of forces acting on individual grains within a soil matrix. Some of the potential forces are involved in the mobilization process including self-weight, buoyancy, hydrostatic fluid pressure, inter-particle contacts and electrical forces, rotational resistance, and shear forces (Briaud et al., 2008; Fournier et al., 2005; Santamarina, 2001; Kermani et al., 2017). A simplified example illustrating some of these forces is shown in Figure 2-5, including lift force, F_L, and drag force, F_d, and the force tending to resist mobilization is frictional in nature, F_f. Bedrikovetsky et al. (2011) concluded that if the rotational moments caused by the mobilizing forces, M_m, exceed the resisting moments caused by the retention forces, M_R, a soil particle will become detached and eroded. Figure 2-4 presents a generalized interpretation of the orientation and magnitude of these forces and moments.

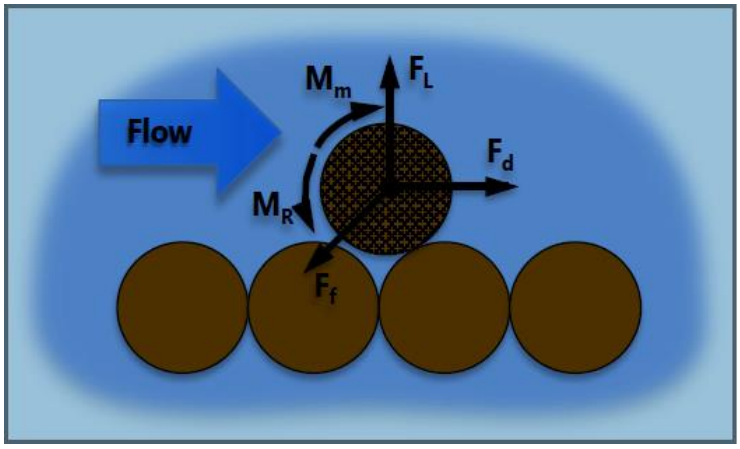

Figure 2-4. Simplified schematic diagram outlining the interaction of forces during particle mobilization. (Xiao et al., 2018)

Studies were conducted to determine the mechanisms of release. For example, Sharma et al. (1992) conducted experiments to study the various factors (pH, ionic strength, flow rate, surface material and roughness) that controlled the release of particles from flat surfaces and particle release mechanism. The experiments were set to determine which mechanism (rolling or sliding) dominated the particle release. The flow and centrifuge experiments were used to determine the flow rates. The velocity at which an observed 10% of the particles releasing from the surface were referred as the critical velocity. It turned out that the hydrodynamic forces had the following relationship with particle properties and flow rate.

$$V_x = 6(Q/A)(R/l)(1 - (R/l)) \quad (6)$$

where Q = the flow rate; R = the average particle diameter; A = the cross-sectional area of the flow channel; and l = the space between the two plates (Sharma, et, al., 1992).

2.2.2 Particle Transport and Deposition

The ability for particles to migrate through the porous media depends on several factors: the permeating fluids and the suspend particles (Baghdikian et al., 1989). Common knowledge of particle deposition is well documented in the literature. The traditional criteria for soil filters are based on empirically derived ratios corresponding to base soil and filter soil particle sizes (Bertram, 1940; Lund, 1949; Terzaghi, 1943; USACE, 1971). Sherard et al. (1984a) concluded that for cohesionless sand and gravel, the D_{15} of a filter gives a quantitative measure of the pore sizes that restrict soil particles from passing through the porous media. Critical filters for cohesive soils were also studied by Sherard et al. (1984b) amongst others (Lowe, 1988; Vaughan and Soares, 1982). The no erosion filter (NEF) test (Sherard, 1989) resulted in the discovery of a filter boundary, D_{15b}, which was unique to each soil type in the study including fine silts and clays, sandy silts and clays, silty and clayey sands with low fines content, and clayey and silty sands.

Several flow pump experiments on a sand and kaolinite mixture were conducted to investigate how important the parameters (critical shear stress, erosion rate) were in the internal erosion process (Reddi et al., 2000a). Flow rate was controlled during the experiments. Distilled water and a sodium chloride prepared at a concentration of 0.001-N and 0.01-N were used as the permeating fluids in the experiments. For the internal erosion investigation, permeants were pumped through an intact soil specimen in a compaction permeator; and for the surface erosion investigation, permeants were pumped through a 7-mm hole preformed within a cylindrical soil specimen. It turned out that critical shear stress increases as the salt concentration increases.

Past literatures defined multiple factors that favored particle migration and deposition. However, the ability to determine which factor or combination of factors governs particle fate under a given set of circumstances is still unclear. Permeating fluids of various suspended particle types, concentrations, viscosity, levels of pH, and ionic strength are essential to a better understanding of the interactions that govern a particle's fate.

2.3 Review of Internal Erosion Affected by Permeating Fluids

In the typical experimental studies such as the pinhole erosion tests, hole erosion tests, and slot erosion tests, tap water or de-ionized water is used as permeating fluid. In the field, permeating fluids through earthen dams or levees may contain particulate matters of various sizes and concentrations, and the fluid's physicochemical characteristics such as viscosity (due to temperature variation and particulate concentration), ionic strength (due to seawater invasion), and pH can be significantly different from those of tap water. The seepage may contain fine particulates that are entrained in the pore fluid from the upstream soils erosion. The particulate matters in the seepage can also contribute to the variations of the physicochemical characteristics of the permeating fluids and consequently may affect the progression of an existing piping channel. The studies conducted by Hubbe (1985, 1987), Sharma et al. (1992), and McDowell-Boyer (1992) attempted to understand the hydrodynamic forces that are required to dislodge particles from flat surfaces. These studies pointed out that the hydrodynamic forces vary with flow rate, particle size, particle elasticity, ionic strength, pH, and the London-van der Waal forces and electrical double

layer forces between colloidal particles and the surface of the solid matrix. They concluded larger particle size, lower pH, and higher ionic strength increase the critical hydrodynamic force required for particle dislodging, i.e., result in less erosion. The literature review and experiments by McDowell-Boyer (1992) provided the quantification of the electrical double layer forces and London-van der Waal forces and related them to the colloids mobilization under laminar flow at flow velocity of 0.001–0.1 cm/sec. An earlier study by Visser (1972) pointed out that tangential force contributes to the dislodging force acting on a particle, while the lift force contributes negligibly to the dislodging force. Annandale (2007), based on the Shields diagram (Shields, 1936), illustrated that the commonly held belief that soil erosion is caused by shear stress is only valid in laminar flow; while in turbulent flow, normal lift force dominates. Previous researchers also conducted erosion tests on soil columns using permeating fluids of varying ionic strength. Sherard et al. (1972), Arulanandan et al. (1975), and Reddi et al. (2000) reported that higher content of dissolved salts in the water (i.e., higher ionic strength) resulted in lower erosion of clayey soil.

Past research along with the preliminary HET tests by the authors showed that soil's erosion behavior is influenced by the physicochemical characteristics of fluids. Meanwhile, these characteristics of fluids can interact with either other in affecting the soil's erosion behavior. Xiao et al. (2018) studied the incipient motion of a single spherical glass bead subjected to fluids of various combinations of viscosity, ionic strength, and pH under laminar flow and found that viscosity, pH, and their two-way interaction were the most influencing factors on critical velocity for particle mobilization, and the effects of the three fluid characteristics on critical velocity follow the following decreasing order: viscosity,

pH, and ionic strength. In this experimental research, we aimed to address an important question that has not been answered by previous research, i.e., how viscosity, ionic strength, and pH individually and collectively affect the piping progression of a sandy soil under turbulent flow conditions.

CHAPTER 3 RESEARCH MATERIALS AND MATHODOLOGY

3.1 Experimental Setup

The experimental research employed the hole erosion test (HET). In the series of experiments, a sandy soil was prepared. The soil was an engineered fill and sieved through U.S. #20 sieve (0.84 mm), the portion that passed #20 sieve was then added with 6% (by mass) of Kaolin clay. The soil has D_{50} = 0.24 mm, liquid limit = 10.6, and plasticity index = 4. It is classified as SW (well-graded sand) according to the Unified Soil Classification system. The soil was reconstituted in a specially designed Plexiglas flow cell as shown in Figure 3-1. The diameter of the soil specimen after compaction was 7.0 cm (2.75 inch) and its length was 7.6 cm (3 inch). Figure 3-2 shows the experimental setup. Fluid was provided to the flow cell by an upstream constant-head reservoir while a downstream constant-head reservoir received the flow cell's effluent. The fluid was circulated from the downstream reservoir back to the upstream reservoir using a submersible pump. The hydraulic head difference was controlled by raising or lowering a mechanical jack that supported the upstream reservoir. A flowmeter was used to constantly record the flow rate variations during the test. In order to measure the hydraulic gradient across the soil specimen, two tubes (manometers) were connected with the flow cell and were used to measure the head difference across the soil specimen during the erosion testing.

Figure 3-1. Flow cell for soil specimen

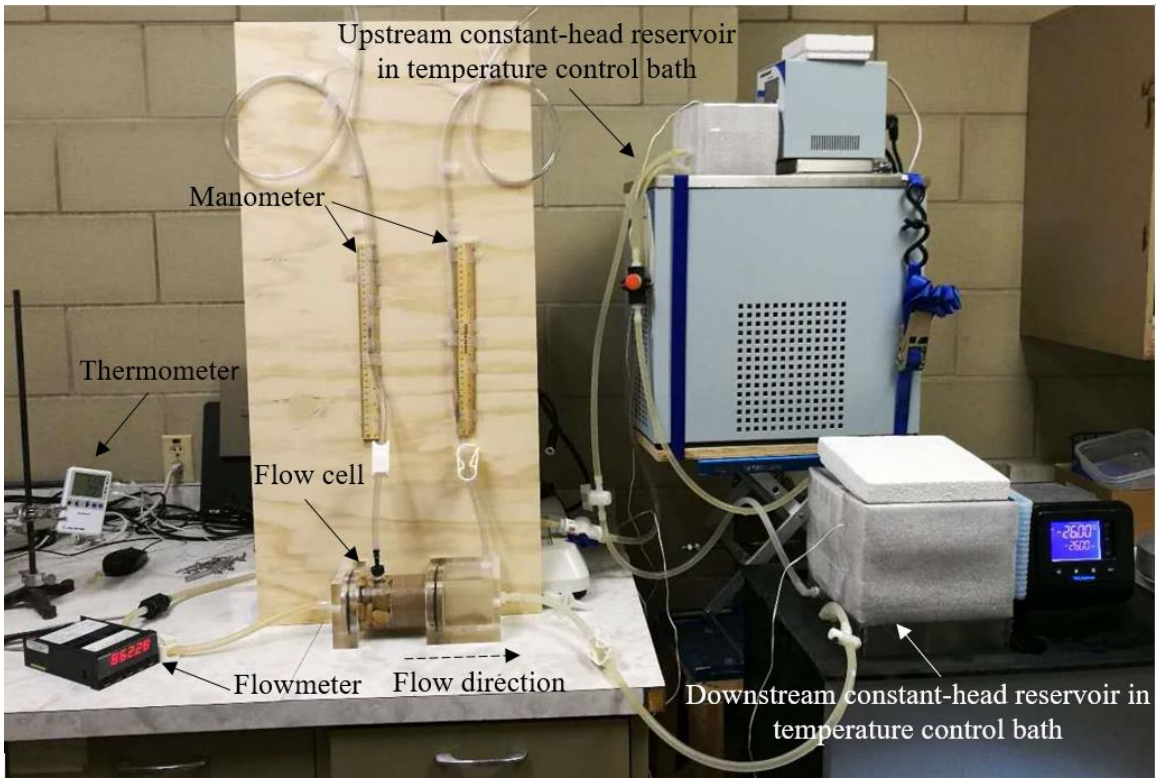

Figure 3-2. Experimental setup of hole erosion test

3.2 Design of Experiments and Fluid Preparation

Three physicochemical characteristics (factors) of fluid were studied: pH, ionic strength, and viscosity. Distilled water was used as the base of each test fluid. Each fluid parameter has a target low and high levels as shown in Table 3-1. The highest and lowest values of temperature that can be obtained from the fluids are 50.00 °C and 7.00 °C. The ionic strength of the sea water is around 0.7 mol/L and the ionic strength of the tap water is about 0.05 mol/L. Using full-factorial experimental design, the number of fluid types is: $(\text{number of levels})^{\text{number of factors}} = 2^3 = 8$. The three-factor, two-level, full factorial design and preparation of the experimental fluids are listed in Table 3-2. The fluid preparation follows the following three steps.

Table 3-1. Two levels of fluid's physicochemical properties

Fluid properties	**Low level**	**High level**
Viscosity: μ (g/cm·s = Poise)	0.0054 (at 50.00°C)	0.0142 (at 7.00°C)
pH: *P*	3.5 (add HCl)	10.50 (add NaOH)
Ionic strength: *I* (mol/L)	0.05 (add NaCl)	0.5 (add NaCl)

Table 3-2. Three-factor, two-level, full factorial design and preparation of the experimental fluids

Fluid number	**Fluid descriptions**	**Fluid temperature (°C)**	**Acid or base in 13 L of fluid (g)**	**NaCl in 13 L of fluid (g)**
1	Low μ, low *P*, low *I*	50.00	4.133 (HCl)	37.866
2	Low μ, low *P*, high *I*	50.00	4.133 (HCl)	379.740
3	Low μ, high *P*, low *I*	50.00	0.900 (NaOH)	37.328
4	Low μ, high *P*, high *I*	50.00	0.900 (NaOH)	379.202
5	High μ, low *P*, low *I*	7.00	4.189 (HCl)	37.866
6	High μ, low *P*, high *I*	7.00	4.189 (HCl)	379.740
7	High μ, high *P*, low *I*	7.00	0.030 (NaOH)	37.959
8	High μ, high *P*, high *I*	7.00	0.030 (NaOH)	379.833

3.2.1 Adjust Viscosity

The target viscosities were achieved by adjusting the temperature of the fluid using the upstream and downstream temperature control baths. The targeted temperatures were selected based on the assumption that each fluid would follow the well-established relationship between the temperature of distilled water and its corresponding viscosity, as described graphically in Equation (7) (Al-Shemmeri, 2012).

$$\mu = 2.414 \times 10^{-6} \times 10^{247.8/(T-140)} \quad (7)$$

where: μ is dynamic viscosity (Poise, or g/(cm·sec)), T is temperature (in Kelvin). Equation (7) applies to temperature from 0 °C to 370 °C. This technique of using temperature to adjust viscosity allowed simultaneously adjusting the three characteristics to their target values according to the experimental design methodology. To accurately control the fluid temperature (and thus, viscosity) both the upstream and downstream fluid reservoirs were placed in temperature control baths. The actual temperature of the test fluid in each test was approximated using the average of temperature measurements taken in the upstream and downstream reservoirs.

3.2.2 Adjust pH

The pH was lowered to a targeted value by adding an appropriate quantity of hydrochloric acid (HCl) and raised to a targeted value by adding an appropriate quantity of sodium hydroxide (NaOH). HCl and NaOH are examples of a strong acid and base, respectively, which are known to dissolve completely in water and therefore yield reliable concentrations of hydrogen ions (thus pH) at equilibrium (Benjamin, 2010). Adjustment of pH considered the temperature effect. The dissociation constant of water (K_W) changes with temperature as shown in Equation (8) and consequently affects pH.

$$pK_w = 14.9429 - 0.043126 \times T + 0.0002291 \times T^2 - 0.000000782 \times T^3 \quad (8)$$

where $pK_w = -\log(K_w)$, and T = temperature in Celsius.

The molar concentration of $[H^+]$ and $[OH^-]$ needed to achieve the desired pH can be calculated based on Equations (9) and (10), respectively:

$$[H^+] = 10^{-pH} \quad (9)$$

$$[OH^-] = K_w/[H^+] \quad (10)$$

If $[H^+] > [OH^-]$, then HCl needs to be added to the fluid. If $[H^+] < [OH^-]$, then NaOH needs to be added. In this research, commercially available HCl solution with 3.65% mass concentration (1 molar/liter) was used; such solution has density of 1.0189 g/ml at 5 °C and 1.0054 g/ml at 50 °C. NaOH is in the form of solid pellet. The following two formulae are used to determine the amounts of acid and base required to achieve the target $[H^+]$ and $[OH^-]$ concentration as determined in Equations (9) and (10).

Concentration of HCl (gram per liter of final solution) = solution's density (in g/ml) $\times 1000 \times ([H^+] - [OH^-])$ (11)

Concentration of NaOH (gram per liter of final solution) = $40 \times ([OH^-] - [H^+])$ (12)

3.2.3 Adjust Ionic Strength

Sodium chloride (NaCl) was used to adjust the solution to the desired ionic strength. The ionic strength depends on the concentrations and valences of ions in the solution, as shown in Equation (13) (Benjamin 2010):

$$I = \frac{1}{2} \sum_{\text{all ions}} (c_i z_i^2)$$

$$= \frac{1}{2}\{[\mathrm{Na}^{+1}] \times 1^2 + [\mathrm{Cl}^{-1}] \times (-1)^2 + \mathrm{ABS}([\mathrm{H}^{+1}] - [\mathrm{OH}^{-1}] \times 1^2)\}$$

$$= \frac{1}{2}\{[\mathrm{NaCl}] \times 2 + \mathrm{ABS}([\mathrm{H}^{+1}] - [\mathrm{OH}^{-1}])\} \quad (13)$$

So: $[\mathrm{NaCl}] = I - 0.5 \times ABS([\mathrm{H}^{+1}] - [\mathrm{OH}^{-1}])$ (14)

where I = ionic strength of the solution, c_i = concentration of the i^{th} ionic species, z_i = charge on the i^{th} ionic species, and $[Na^{+1}]$, $[Cl^{-1}]$, [NaCl], $[H^{+1}]$, $[OH^{-1}]$ represent the molar concentrations of Na^{+1}, Cl^{-1}, NaCl, H^{+1}, OH^{-1}, respectively. The effect of salt concentration (up to 0.5 mol/L in this research as shown in Table 2) on viscosity was neglected in this study. Zhang and Han (1996) measured the viscosity of water with NaCl solution at 25 °C, the data showed the dynamic viscosity increased by 4.67 % when the ionic strength increased from 0 to 0.5 mol/L. With a target ionic strength (I), the molar concentration of NaCl per liter can be determined by Equation (14). The mass (in gram) of NaCl per liter of solution is [NaCl] ×58.44.

3.3 Experimental Procedure

For each of the 8 fluids, two repeat tests were conducted after each specific fluid was prepared in the upstream and downstream reservoirs at target temperature (thus viscosity), pH, and ionic strength. The soil was compacted in three uniform layers at 95% of the maximum dry density (ρ_{dmax} = 2.10 g/cm^3) at the optimum water content of 11% (based on the standard proctor test). A hole was formed in the middle of the specimen using a drill; the initial hole diameter was 2.5 mm. Filter papers were attached to both surface of

the soil specimen, a hole was cut in the filter paper to allow eroded particles to exit the soil specimen without impedance. Gravels were used to fill the upstream space of the flow cell. The upstream and downstream reservoirs were initially connected without the flow cell to circulate the fluid to achieve uniform temperature in the system. Then the soil specimen was saturated using the fluid by positioning the soil specimen in vertical orientation and slightly pushing the fluid upward in the specimen to expel the air. After soil saturation, the flow cell was positioned in horizontal orientation, and a control valve was fully opened. During the HET, the head difference and flow rate were measured every 1 minute during the maximum of 90-min duration. After each test, the flow cell was disconnected and allowed to reach to room temperature. Then the soil specimen was carefully extruded and cut into halves. The final diameter of the piping channel was measured at three different locations using a caliper to obtain the average hole diameter.

3.4 HET Data Processing

The erosion rate indexes of the soil under various permeating fluids were obtained to quantify the relative and interactive effects of fluid's physicochemical properties on the fluid's erosive capacity. The HET data processing approach to derive the erosion index followed that of Wan and Fell (2004) and is briefly presented as follows. As previously mentioned in the literature review chapter, $\dot{\varepsilon}_t$ and I_e can be expressed in Equations (2) and (3), respectively.

In the HET data analysis, flow rate was used as an indirect measurement of the diameter enlargement of the pre-formed hole. The hydraulic shear stress along the pre-formed hole can be derived from the Hagen-Poiseuille law and expressed as:

$$\tau_t = \rho_w g s_t \frac{\varphi_t}{4} \tag{15}$$

where: τ_t = hydraulic shear stress (N/m^2); ρ_w = density of the permeating fluid; g = acceleration due to gravity (m/s^2); s_t = hydraulic head gradient; φ_t = hole diameter at time t (m).

Based on the definition of $\dot{\varepsilon}_t$ (kg/s/m^2), it can be expressed as

$$\dot{\varepsilon}_t = \frac{\rho_d}{2} \frac{d\varphi_t}{dt} \tag{16}$$

where ρ_d = dry density of the soil (kg/m^3)

A flow in a piping channel can be laminar flow or turbulent flow. Reynolds Number (R_e) is used to describe the flow regimes. In a full circular pipe flow, if $R_e < 4000$ (Holman, 2002), the flow is dominated by viscous fluid force and is laminar flow; if $R_e > 4000$, the flow is dominated by inertial forces and is turbulent flow. In the HETs, the minimum Reynolds number was 13213, so the flow is turbulent flow. In turbulent flow, φ_t at time t can be estimated using (Wan and Fell, 2004):

$$\varphi_t = \left(\frac{64 {Q_t}^2 f_{Tt}}{\pi^2 \rho_w g s_t}\right)^{1/5} \tag{17}$$

where: f_{Tt} is the friction factor relating the shear stress to the flow velocity in turbulent flow condition, and Q_t= flow rate at time t (m^3/s). f_{Tt} is assumed to vary linearly with time (Wan and Fell, 2004) and can be obtained using the initial and final diameters as well as the measured flow rate using Equation (17). After the function of f_{Tt} and t is obtained,

the relationship between φ_t and t can be determined. Then Equations (15) and (16) are used to compute τ_t and $\dot{\varepsilon}_t$, respectively, as time (t) elapsed. When $\dot{\varepsilon}_t$ is plotted against τ_t, the rising part of the plot can be approximated by a best-fitted straight line, where the slope of the line is C_e, based on Equation (2). The Erosion Rate Index (I_e) can then be determined using Equation (3).

3.5 Regression Analysis of HET Results

A regression model was used to analyze the results in terms of erosion rate indexes of the three-factor, two-level full factorial experiments. The three factors are denoted by *A*, *B* and *C* and the two factor levels are denoted by i =1, 2 (for factor *A*), j =1, 2 (for factor *B*), and k =1, 2 (for factor *C*). For each combination of the three factors with two different values, *r* replicates are conducted, and the design is a completely randomized design with 2×2×2 observations for each group. The appropriate statistical model is the following additive model (Toutenburg, 2009).

$$y_{ijkl} = \mu + \alpha_i + \beta_j + \gamma_k + (\alpha\beta)_{ij} + (\alpha\gamma)_{ik} + (\beta\gamma)_{jk} + (\alpha\beta\gamma)_{ijk} + \epsilon_{ijkl} \ (l = 1, \ldots, r) \quad (18)$$

where:

y_{ijkl} = the response to the ith level of factor *A*, the jth level of factor *B*, and the kth level of factor *C* in the lth replicate;

μ = the overall mean;

α_i = the effect of ith level of factor *A;*

β_j = the effect of jth level of factor *B;*

γ_k = the effect of kth level of factor *C;*

$(\alpha\beta)_{ij}$ = the interaction of the combination of α_i and β_j;

$(\alpha\beta\gamma)_{ijk}$ = the interaction of the combination of α_i and β_j and γ_k;

ϵ_{ijkl} = the random error.

In this research, viscosity, pH and ionic strength are donated by *A, B* and *C*. Two factors level are denoted by *i, j,* and *k,* where $i = j = k$=1, 2. Each test of the different permeating fluid is replicated twice. The total response values will be given in the following section.

3.6 Determination of Soil's Shear Strength under Different Temperatures

This technique of using temperature to adjust viscosity allowed simultaneous adjustments of the three characteristics to their target values according to the experimental design methodology. If using other non-aqueous phase liquids than water to control viscosity, dissolution of acid or basic solutions and salt in such liquids is difficult. Therefore, we controlled temperature to adjust viscosity that can vary three folds in value, while dissolution of acid/basic solutions and salt in water can still be easily achieved. Although such technique proved to be effective when studying the mobilization of an individual particle (Xiao et al. 2018), the temperature variation may alter the soil's erosion resistance. To study the potential effect of temperature on soil's shear strength, which may relate to soil's erosion behavior (Noble and Demirel, 1969), direct shear test was conducted to quantity the shear strength parameters under two temperatures.

Figure 3-3 shows the experimental setup of the direct shear test of soil under controlled temperatures. In the test, water was first heated (or cooled) in the temperature control bath. Then the water was pumped into the direct shear chamber using a hollow copper tube (Figure 3-4). The soil was compacted to the same dry density as in the HETs. Thermocouple and thermometer were used to measure the temperature of water and soil during the test, respectively. 8 °C and 40 °C were set as two temperature levels. 50 kPa, 70 kPa and 100 kPa were used as different vertical stress levels during the tests. Mohr-Coulomb failure criterion line was obtained from the test points for a certain temperature and the cohesion and friction angle were determined.

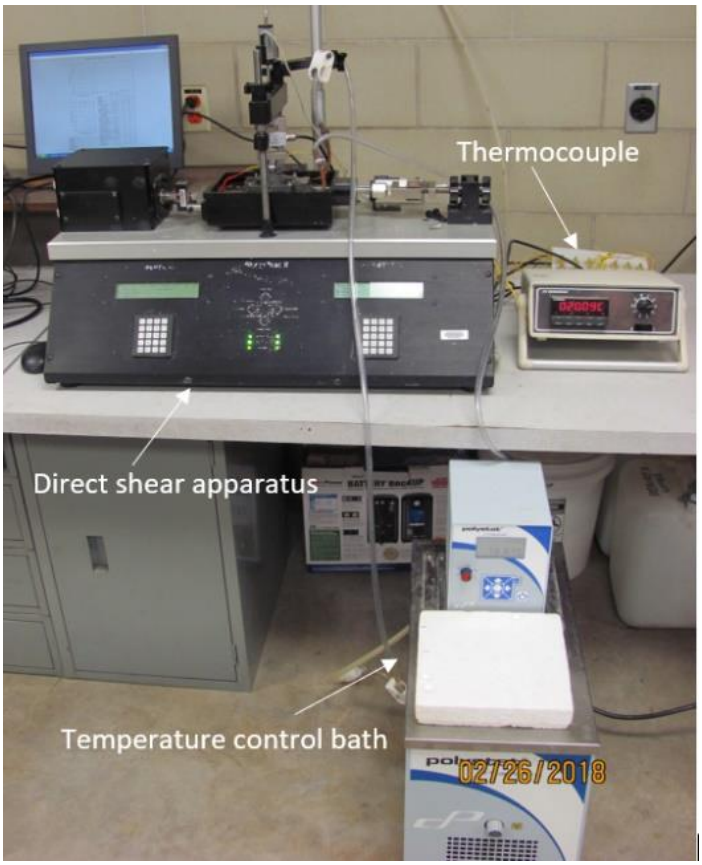

Figure 3-3. Experimental setup of direct shear test of soils under different temperatures

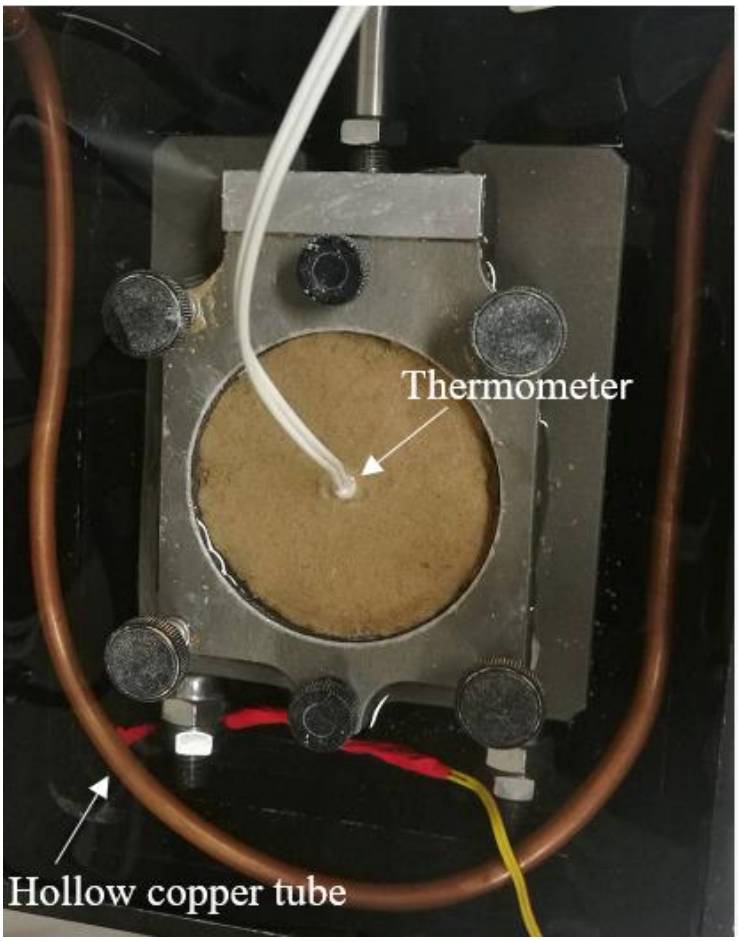

Figure 3-4. Copper tube that circulates water of a target temperature in the direct shear chamber

CHAPTER 4 RESULTS AND ANALYSIS

4.1 Results of Erosion Rate Index Calculation

The approach of determining erosion rate index is illustrated with one permeating fluid (i.e., high viscosity μ, low pH, low ionic strength I). Figure 4-1 shows the measured flow rate variation with time during the HET. Figure 4-2 shows the measured hydraulic gradient variation with time. For each fluid, two identical tests (denoted as Test 1 and Test 2) were conducted to verify the repeatability. Based on the initial and final flow rates and the measured hole diameters, the assumed linear relationship between the friction factor f_{Tt} and time t for Test 1 can be estimated as:

$$f_{Tt} = 0.00211t + 10.291 \quad (19)$$

Given the variations of flow rate Q_t, hydraulic gradient S_t, and friction factor f_{Tt} with time t, the variation of hole diameter φ_t with time t can be obtained using Equation (18) and was plotted in Figure 4-3. The equation of the fitted curve for Test 1 can then be estimated as:

$$\varphi_t = 1.017\text{E-}14t^3 - 1.575\text{E-}10t^2 + 1.176\text{E-}06t + 2.491\text{E-}03 \quad (20)$$

The derivative of Equation (20) is taken and combined with Equations (15) and (16), and the relationship between $\dot{\varepsilon}_t$ and τ_t is plotted in Figure 4-4. The coefficient of soil erosion C_e can be estimated by the slope of the best-fitted line, which is shown in Figure 4-4. The erosion rate index, I_e, can be determined by applying Equation (3).

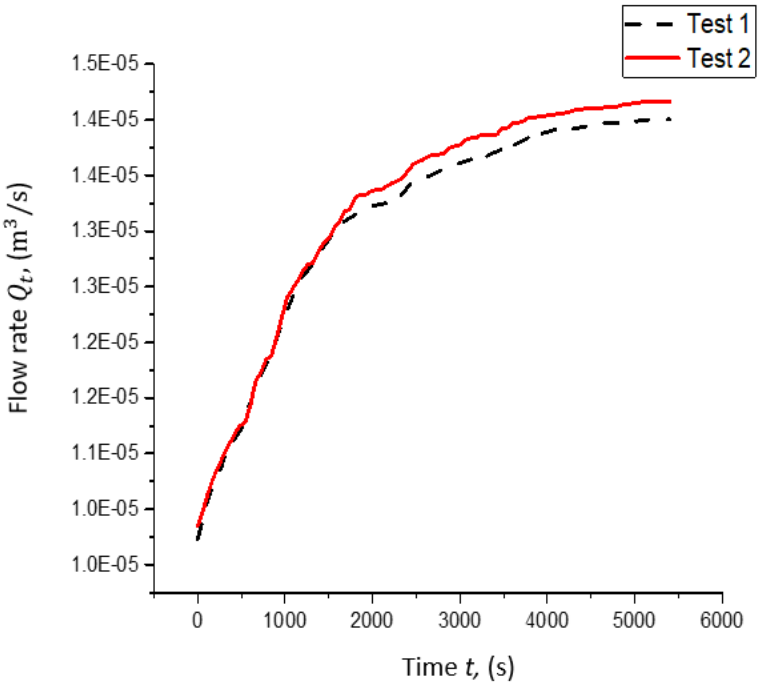

Figure 4-1. Flow rate Q_t vs Time t (High μ, low pH, low I)

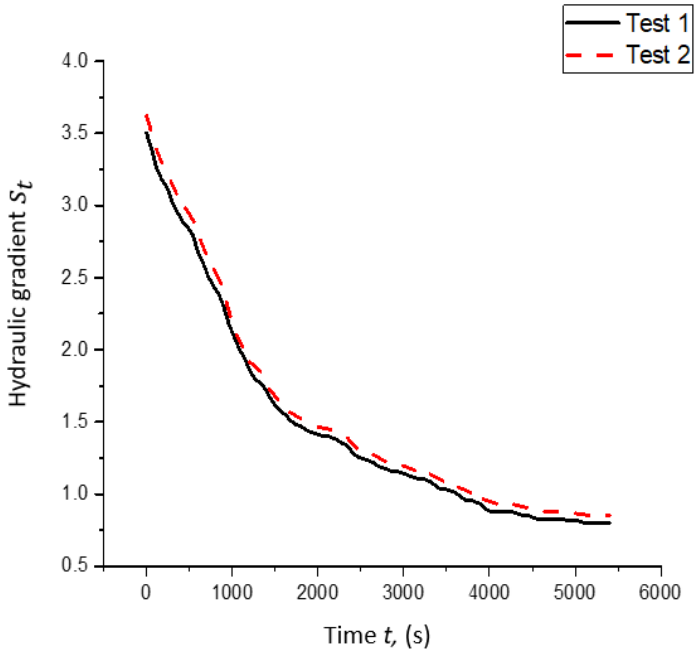

Figure 4-2. Hydraulic gradient S_t vs Time t (High μ, low pH, low I).

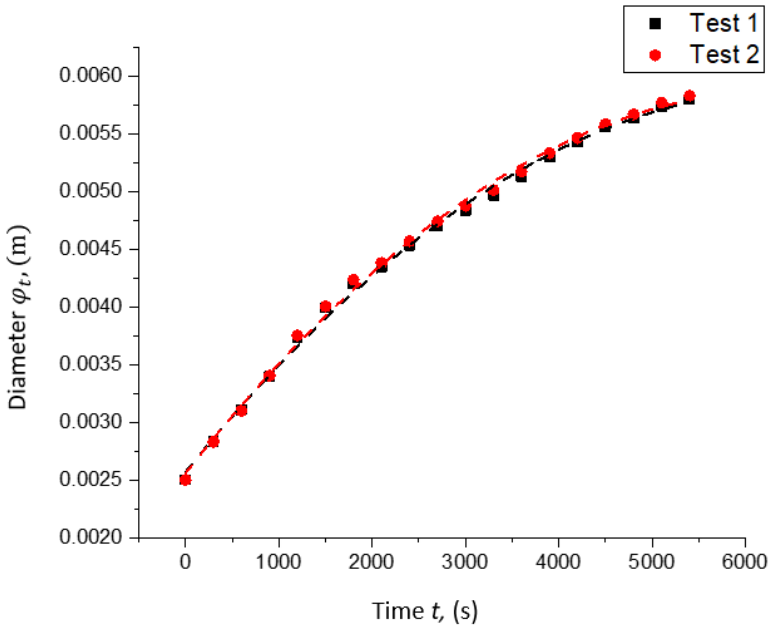

Figure 4-3. Diameter φ_t vs Time t (High μ, low pH, low I).

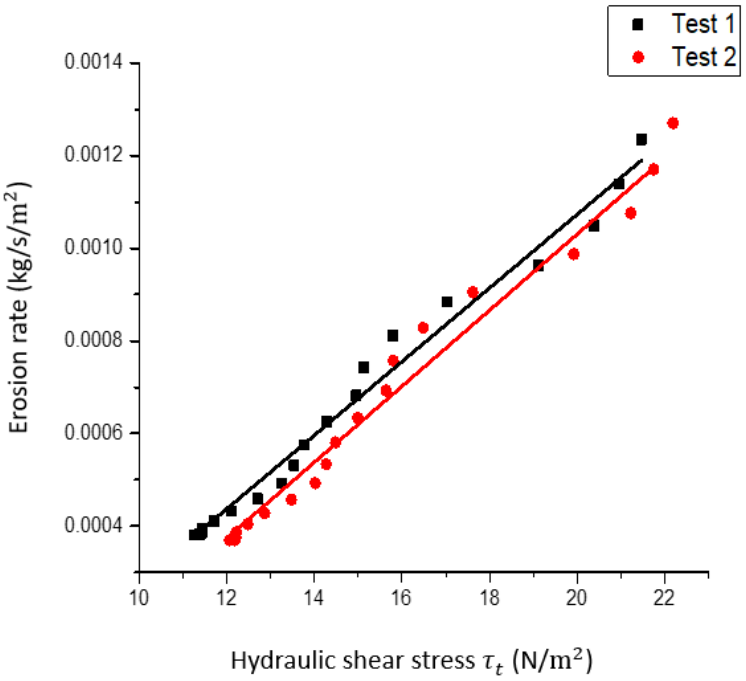

Figure 4-4. Erosion rate $\dot{\varepsilon}_t$ vs Hydraulic shear stress τ_t (High μ, low pH, low I)

The erosion rate index calculations of permeating fluid with *high* μ*, high pH, low I* are shown in Figures 4-5 to 4-8.

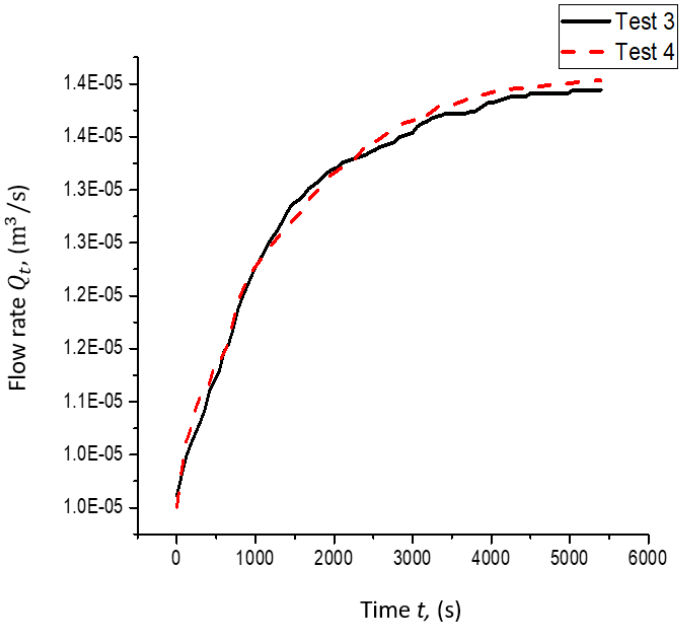

Figure 4-5. Flow rate Q_t vs Time t (High μ, high *pH*, low *I*).

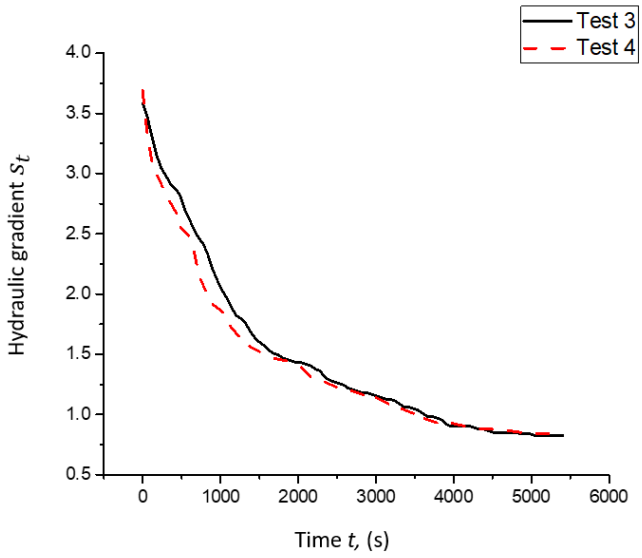

Figure 4-6. Hydraulic gradient S_t vs Time t (High μ, high *pH*, low *I*).

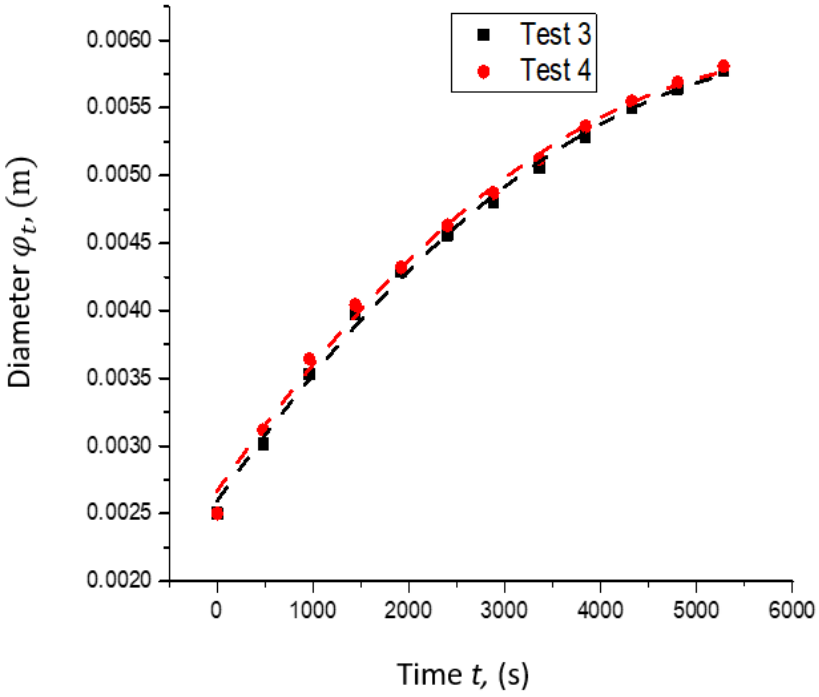

Figure 4-7. Diameter φ_t vs Time t (High μ, high pH, low I).

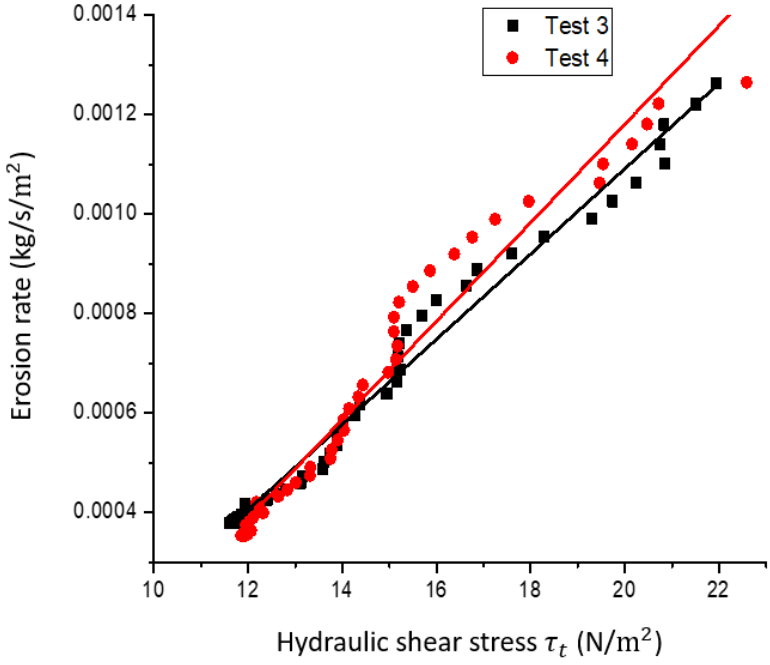

Figure 4-8. Erosion rate $\dot{\varepsilon}_t$ vs Hydraulic shear stress τ_t (High μ, high pH, low I).

The erosion rate index calculations of permeating fluid with *high* μ, *high pH*, *high I* are shown in Figures 4-9 to 4-12.

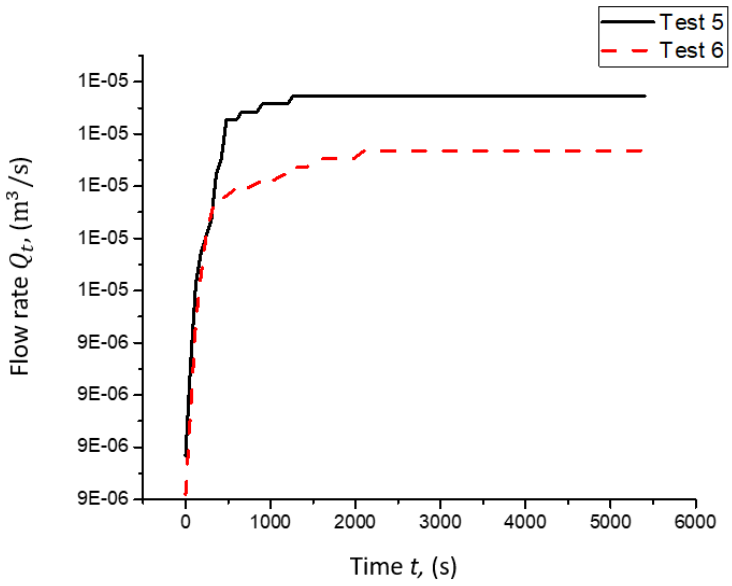

Figure 4-9. Flow rate Q_t vs Time t (High μ, high *pH*, high *I*).

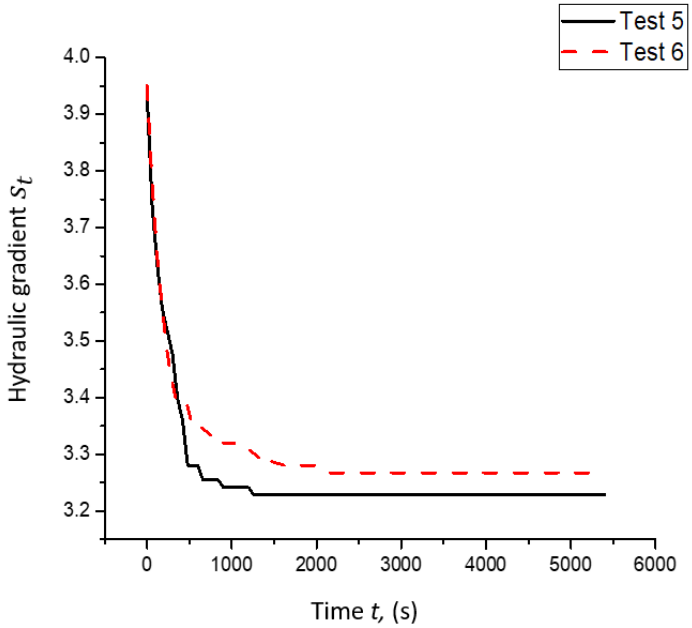

Figure 4-10. Hydraulic gradient S_t vs Time t (High μ, high *pH*, high *I*).

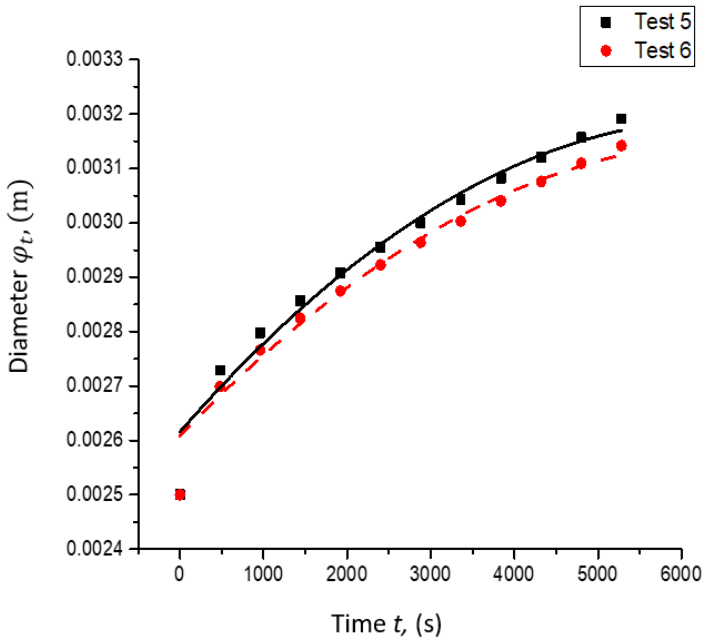

Figure 4-11. Diameter φ_t vs Time t (High μ, high pH, high I).

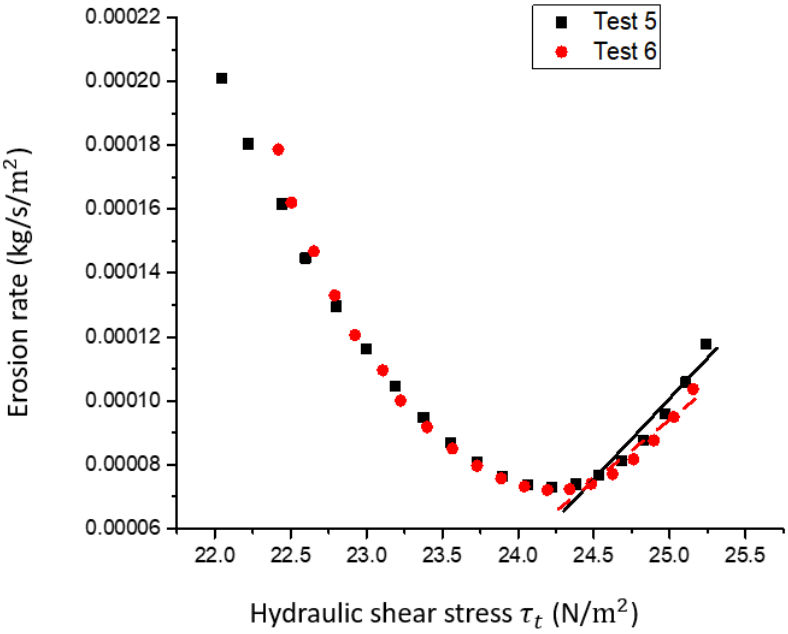

Figure 4-12. Erosion rate $\dot{\varepsilon}_t$ vs Hydraulic shear stress τ_t (High μ, high pH, high I).

The erosion rate index calculations of permeating fluid with *high μ, low pH, high I* are shown in Figures 4-13 to 4-16.

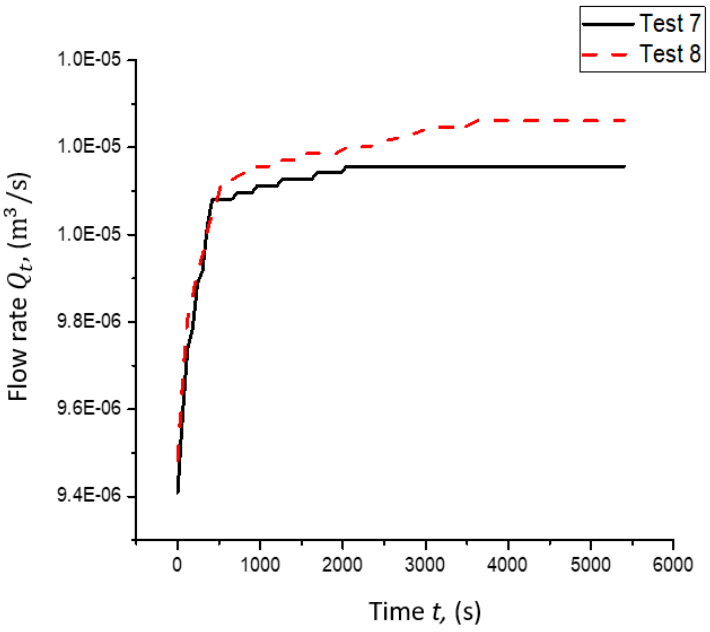

Figure 4-13. Flow rate Q_t vs Time t (High μ, low pH, high I).

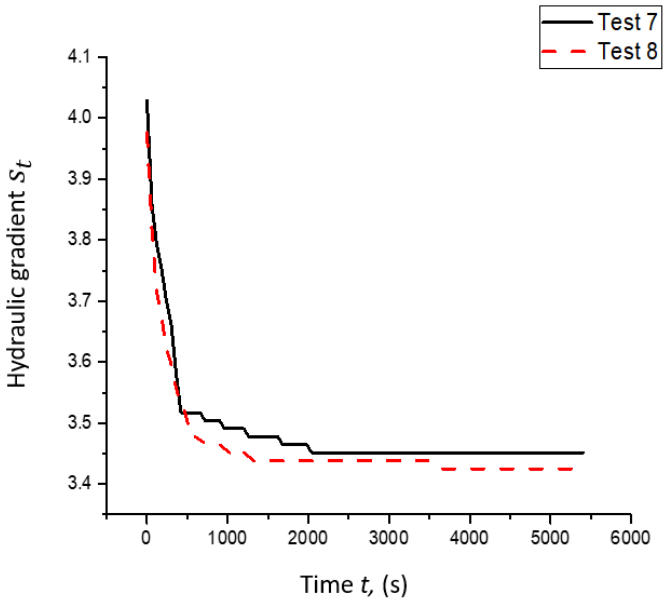

Figure 4-14. Hydraulic gradient S_t vs Time t (High μ, low pH, high I).

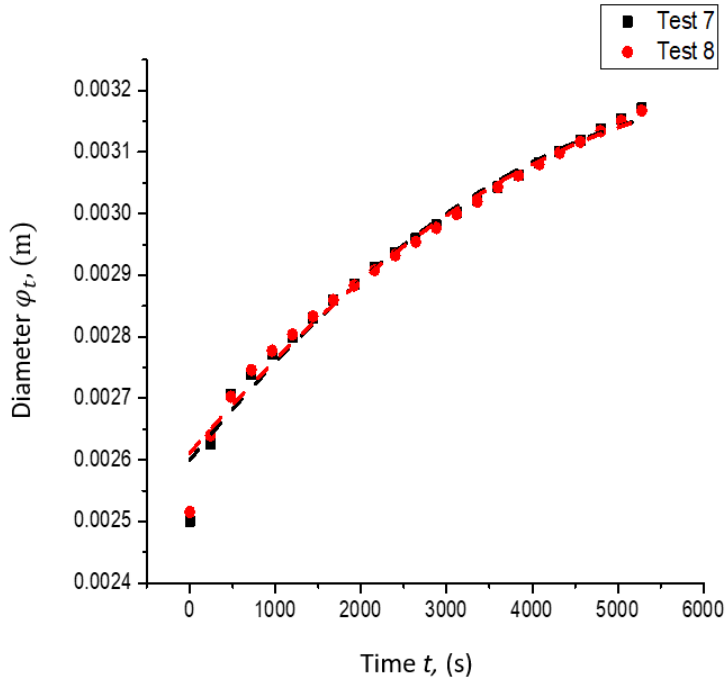

Figure 4-15. Diameter φ_t vs Time t (high μ, low pH, high I).

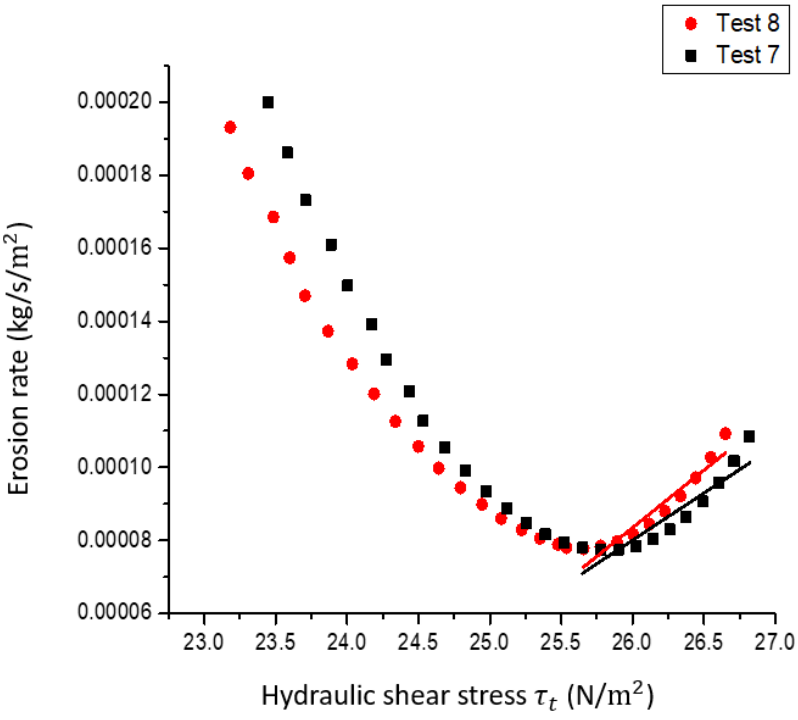

Figure 4-16. Erosion rate $\dot{\varepsilon}_t$ vs Hydraulic shear stress τ_t (high μ, low pH, high I).

The erosion rate index calculations of permeating fluid with *low* μ, *low pH, high I* are shown in Figures 4-17 to 4-20.

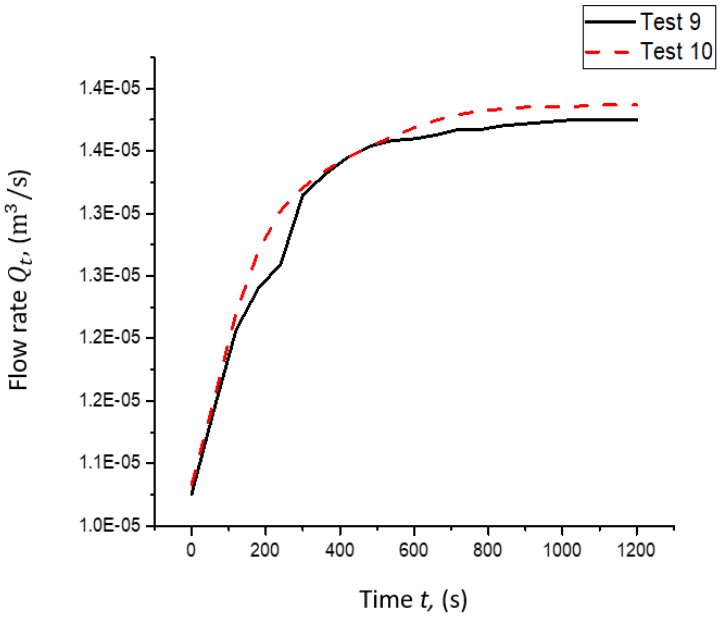

Figure 4-17. Flow rate Q_t vs Time t (Low μ, low *pH*, high *I*).

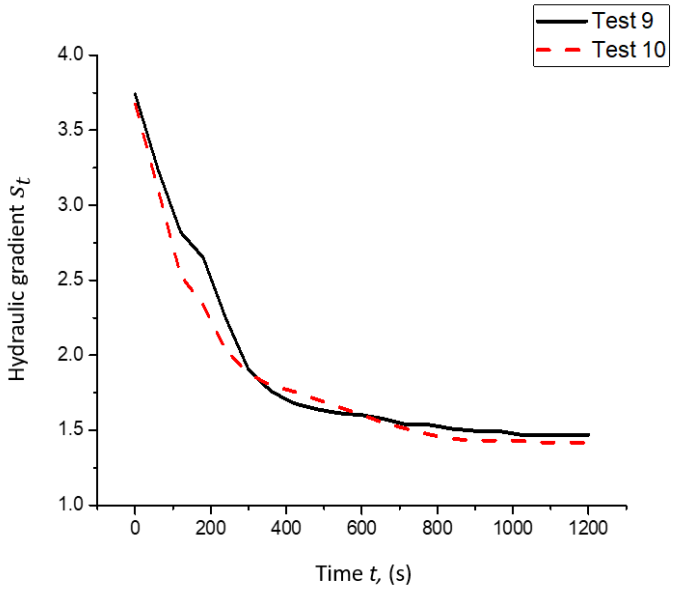

Figure 4-18. Hydraulic gradient S_t vs Time t (Low μ, low *pH*, high *I*).

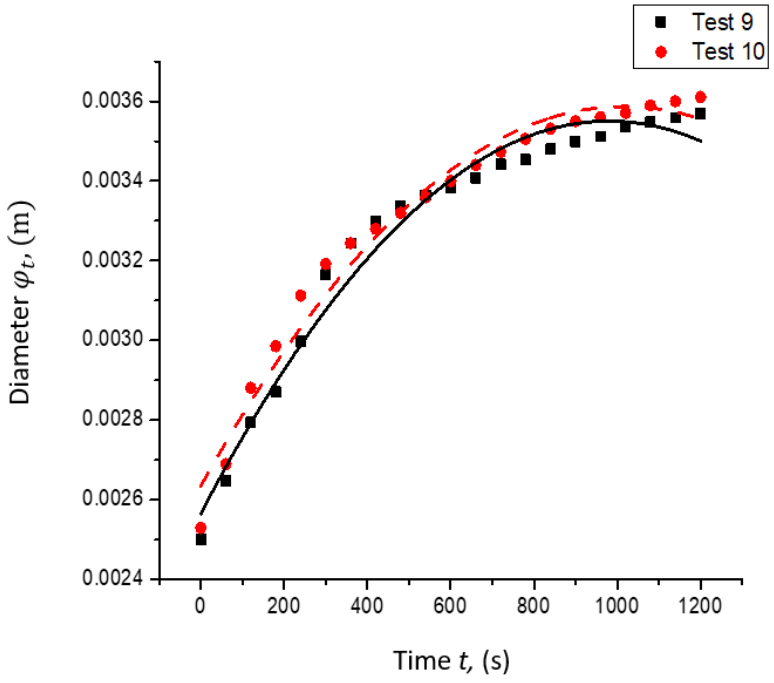

Figure 4-19. Diameter φ_t vs Time t (Low μ, low pH, high I).

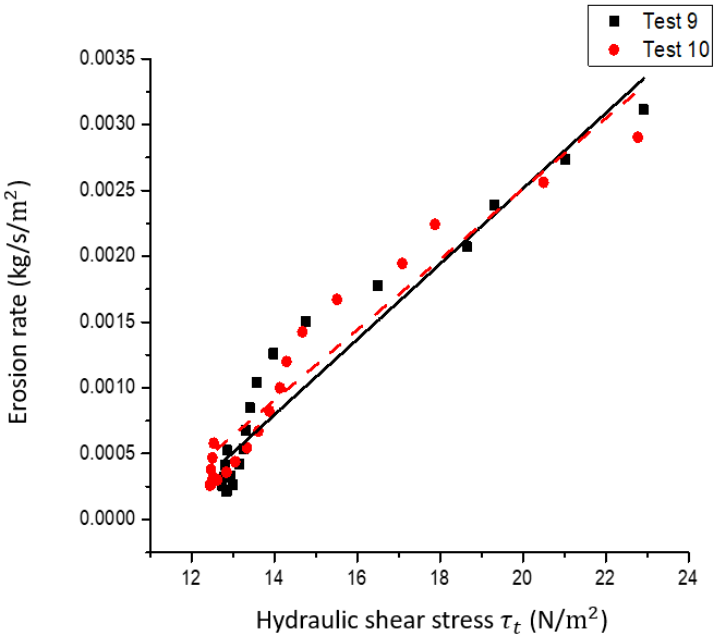

Figure 4-20. Erosion rate $\dot{\varepsilon}_t$ vs Hydraulic shear stress τ_t (Low μ, low pH, high I).

The erosion rate index calculations of permeating fluid with *low* μ, *low pH, low I* are shown in Figures 4-21 to 4-24.

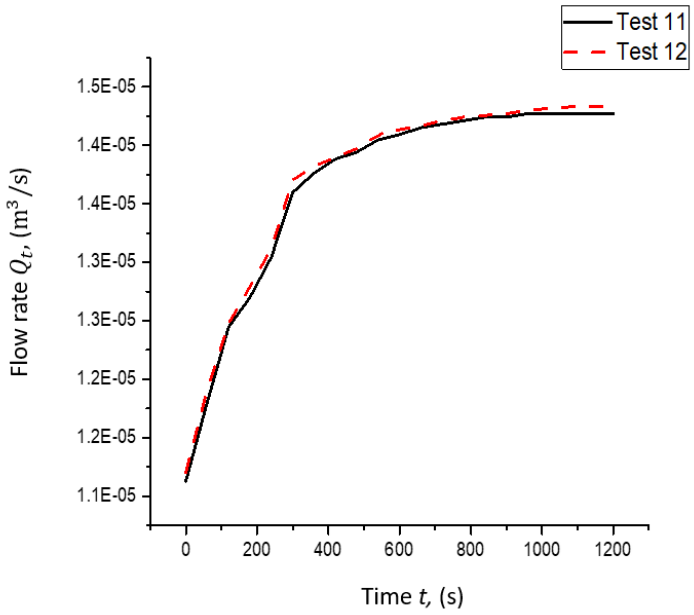

Figure 4-21. Flow rate Q_t vs Time t (Low μ, low pH, low I).

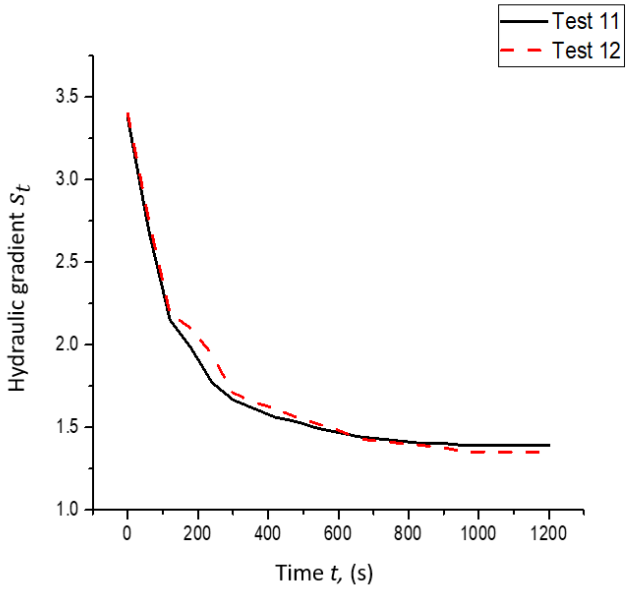

Figure 4-22. Hydraulic gradient S_t vs Time t (low μ, low pH, low I).

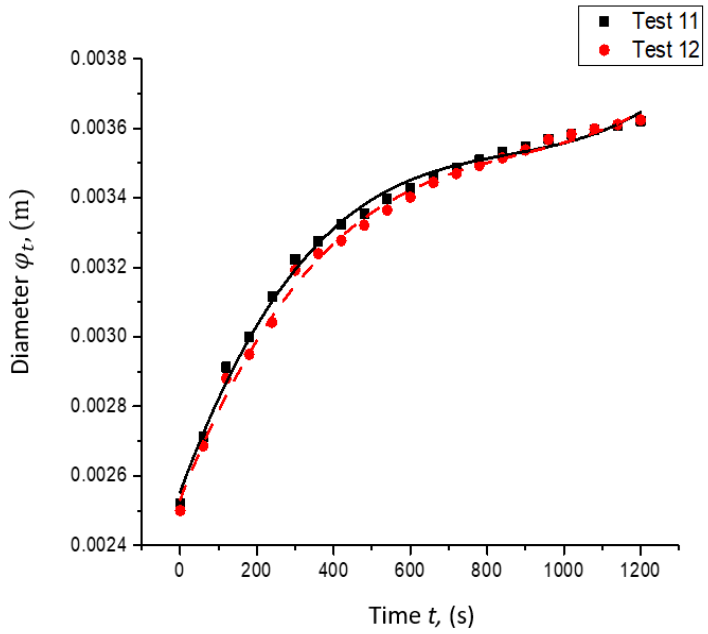

Figure 4-23. Diameter φ_t vs Time t (low μ, low pH, low I).

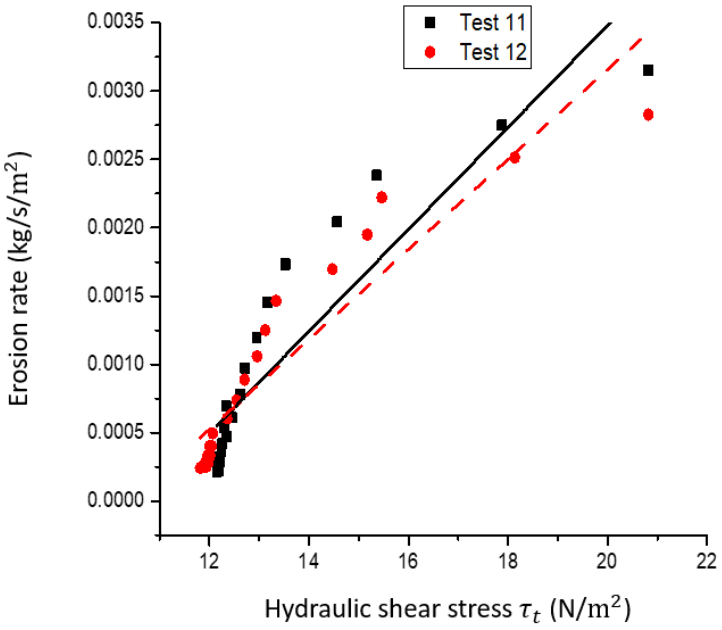

Figure 4-24. Erosion rate $\dot{\varepsilon}_t$ vs Hydraulic shear stress τ_t (low μ, low pH, low I).

The erosion rate index calculations of permeating fluid with *low* μ, *high pH*, *high I* are shown in Figures 4-25 to 4-28.

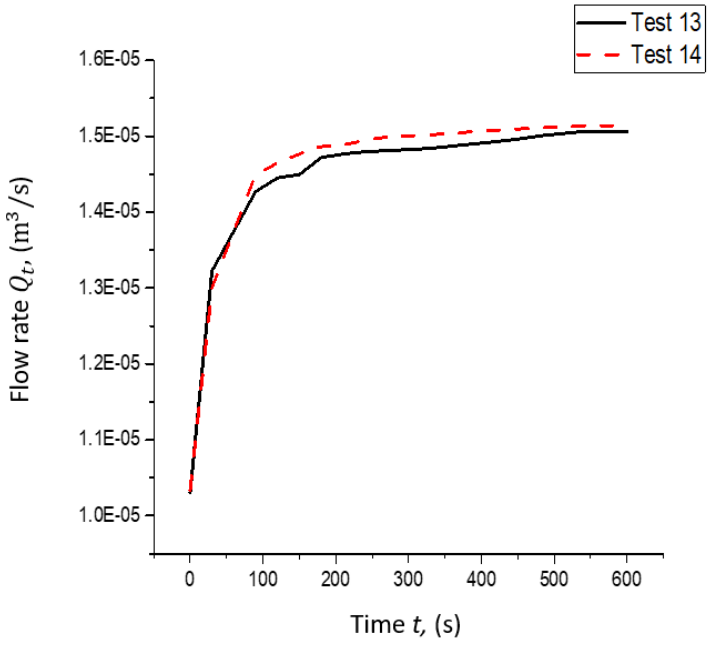

Figure 4-25. Flow rate Q_t vs Time t (Low μ, high *pH*, high *I*).

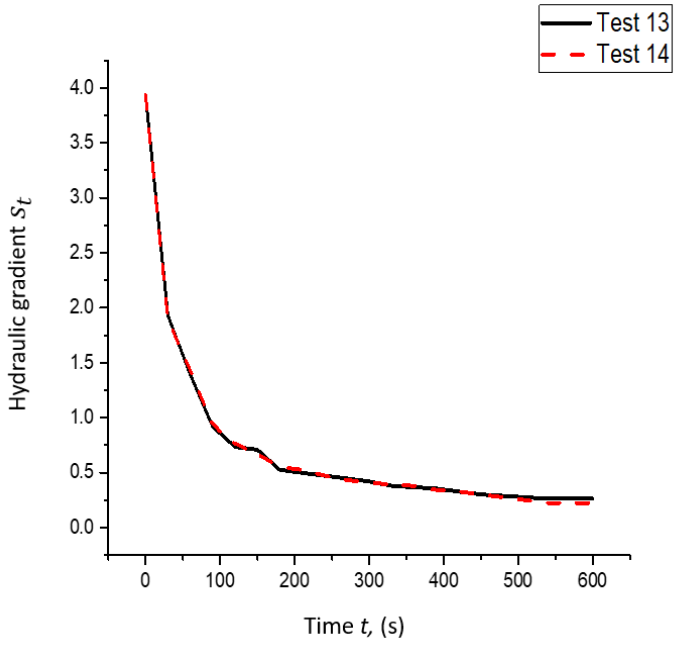

Figure 4-26. Hydraulic gradient S_t vs Time t (low μ, high *pH*, high *I*).

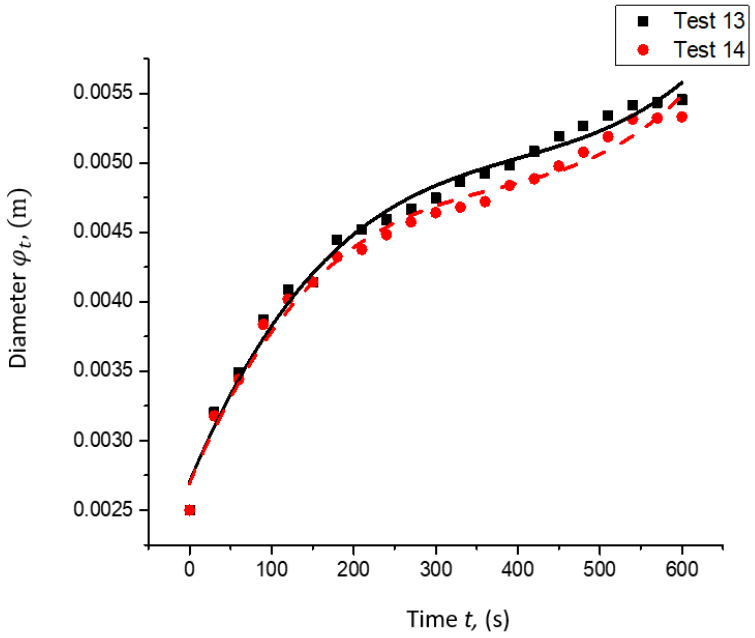

Figure 4- 27. Diameter φ_t vs Time t (low μ, high pH, high I).

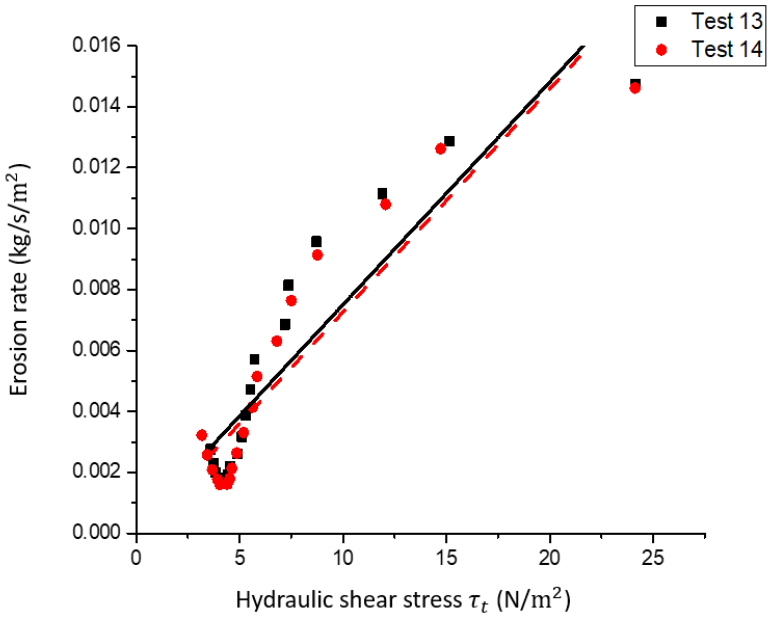

Figure 4-28. Erosion rate $\dot{\varepsilon}_t$ vs Hydraulic shear stress τ_t (low μ, high pH, high I).

The erosion rate index calculations of permeating fluid with *low μ, high pH, low I* are shown in Figures 4-29 to 4-32.

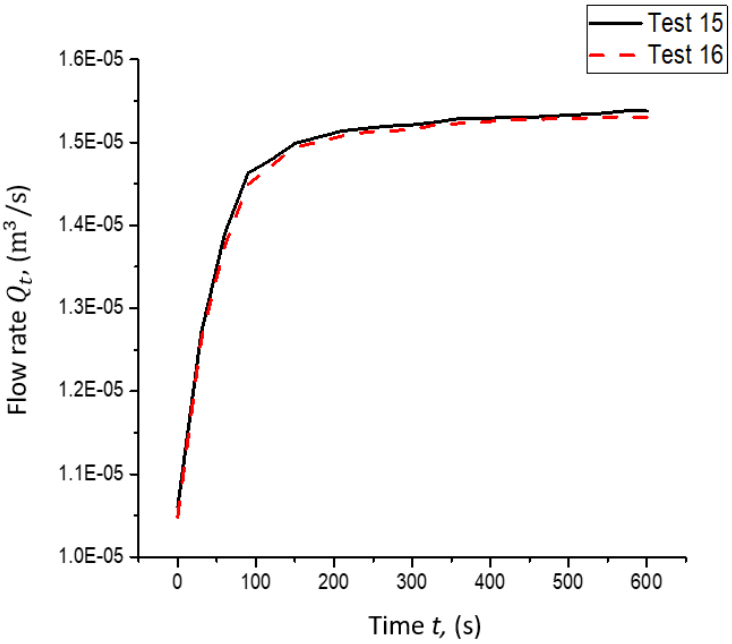

Figure 4-29. Flow rate Q_t vs Time t (low μ, high pH, low I).

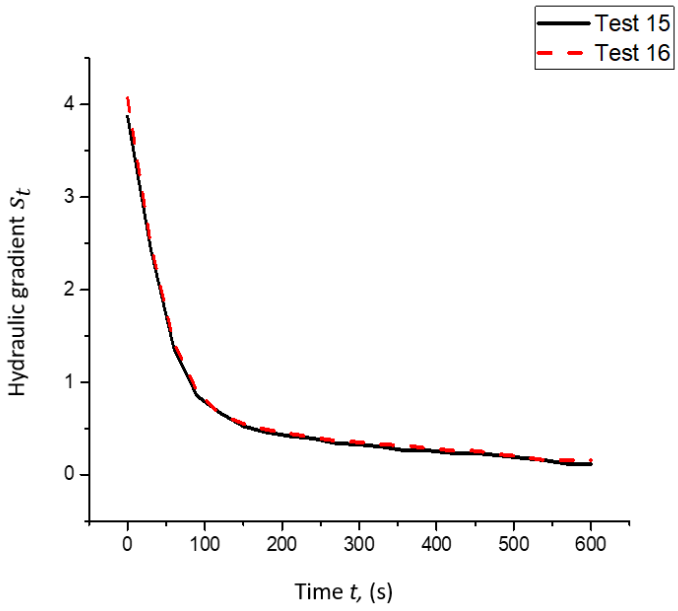

Figure 4-30. Hydraulic gradient S_t vs Time t (low μ, high pH, low I).

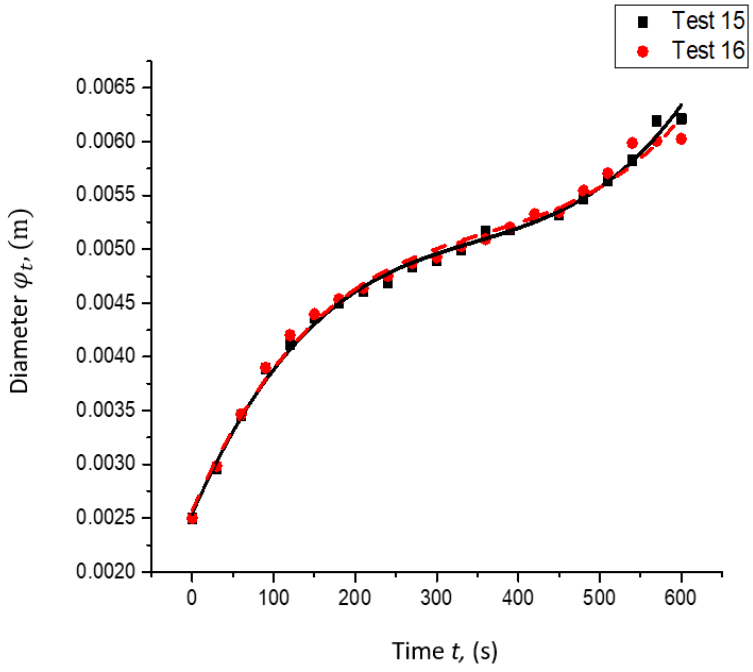

Figure 4-31. Diameter φ_t vs Time t (low μ, high pH, low I).

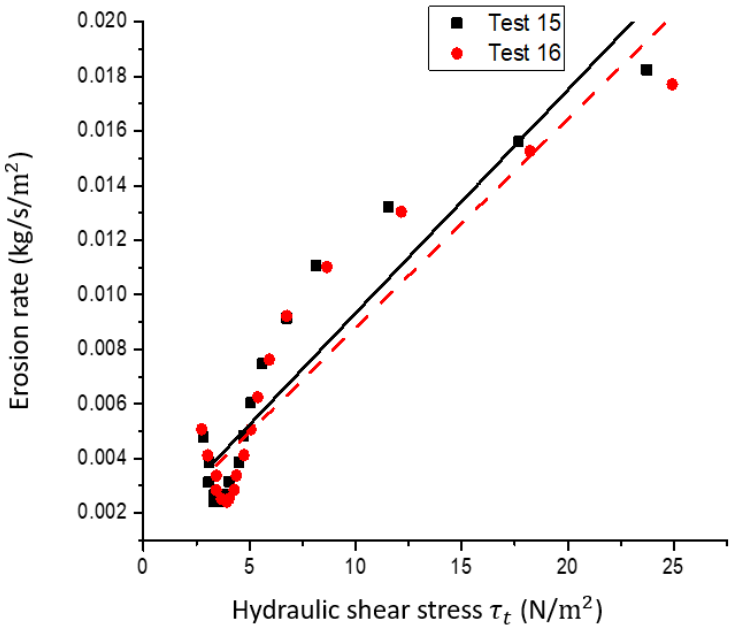

Figure 4-32. Erosion rate $\dot{\varepsilon}_t$ vs Hydraulic shear stress τ_t (low μ, high pH, low I).

Overall, the duplicate tests show good repeatability of the HETs. Table 4-1 shows the determined final erosion rate indexes of the 8 fluids for the two duplicate tests.

Table 4-1. Erosion rate indexes of the 8 fluids

Erosion rate index / Fluids	Test	Duplicate Test	Average
Low μ, low pH, low I	3.45	3.49	3.47
Low μ, low pH, high I	3.56	3.56	3.56
Low μ, high pH, low I	3.09	3.12	3.11
Low μ, high pH, high I	3.17	3.14	3.16
High μ, low pH, low I	4.11	4.09	4.10
High μ, low pH, high I	4.51	4.48	4.50
High μ, high pH, low I	4.07	4.01	4.04
High μ, high pH, high I	4.50	4.38	4.44

4.2 Results of Regression Analysis

ANOVA (analysis of variance) was conducted on the average erosion rate indexes of the 8 fluids. In the analysis, the erosion rate index is known as a response. 95% confidence interval was used for testing the significance of various components.

Table 4-2. Analysis of variance of the erosion rate indexes

Linear Model	Coefficient	*P*-Value
Constant	3.79650	--
μ	-0.47275	0.000
pH	0.10900	0.000
I	-0.11575	0.000
2-Way Interaction		
$\mu \times$ pH	0.008250	0.000
$\mu \times I$	0.008250	0.000
$pH \times I$	-0.00350	0.072
3-Way Interaction		
$\mu \times pH \times I$	-0.00350	0.576

The significance of the effect of viscosity (μ), pH and ionic strength (I) and their interactive effects on the erosion rate index can be judged by the *p*-values in Table 4-2. It can be concluded that viscosity, pH and ionic strength all have significant effect on erosion rate (i.e., *p*-value < 0.0005). Moreover, combined with viscosity, both pH and ionic strength are found to have a strong interaction (i.e., *p*-value < 0.0005), while the interaction of pH and ionic strength has less significant effect (with *p*-value = 0.072 > 0.0005). No significant 3-way interaction among viscosity, pH and ionic strength was captured in this study (with *p*-value = 0.576). In Table 4-2, the coefficient describes the significance (as indicated by the absolute value) and direction (as indicated by the sign) of the relationship between a factor (i.e., viscosity, pH, ionic strength) and the response variable (i.e., erosion rate index). The overall regression function for the erosion rate index is presented in Equation (21).

$$I_e = 3.7950 - (0.47275 \times \mu) + (0.109 \times pH) - (0.11575 \times I) + (0.00825 \times \mu \times pH) + (0.00825 \times \mu \times I) \quad (21)$$

Comparisons of the coefficients in Table 4-2 show that viscosity plays the most important role and ionic strength has slightly more effect than pH on soil erosion. In terms of the interactive effect, when combined with viscosity, both pH and ionic strength have the same interactive effect while pH and ionic strength have the least interactive effect on erosion.

Figure 4-33 quantitatively shows the relative effects of viscosity, pH and ionic strength on the mean response of erosion rate index. When viscosity increased from 0.0054 to 0.142 g/(cm·s) or Poise, the erosion rate index approximately increased from 3.3 (that represents relatively higher erosion) to 4.2 (that represents relatively lower erosion). Such

trend suggests lower viscosity results in higher erosion and conflicts with the understanding as suggested by Equation (22) Kakuturu and Reddi (2006a, 2006b) and the findings by Xiao et al. (2018) under laminar flow conditions

$$\tau(t) = \frac{4Q\mu}{\pi \cdot r_{cc}^3} \quad (22)$$

In the above equation, $\tau(t)$ = hydraulic shear stress acting on a piping channel; Q = flow rate; μ = viscosity of the permeating fluid; r_{cc} = radius of the idealized cylindrical piping channel. This equation suggests under laminar flow, hydraulic shear stress increases with viscosity. Such conflict may be explained in the following two aspects. Based on the Shields diagram (Shields, 1936), Annandale (2007) suggested that the commonly held belief that soil erosion is caused by hydraulic shear stress is only valid in laminar flow, while in turbulent flow normal lift force dominates. Turbulent flow occurred in the HETs in this study. Meanwhile, the soil's resistance to erosion may be affected by temperature, which complicates the quantitative understanding of the relative erosive capacity of the eight fluids. During heating, soil specimen expands, volume increases and pore water pressure also increases (Murayama, 1969; Sherif and Burrows, 1969; Laguros, 1969; Kuntiwattanakul, 1991). Figure 4-34 and Figure 4-35 show the variation of shear stress with horizontal displacement under different vertical stress of 50 kPa, 70 kPa and 100kPa at two temperatures of 8°C and 40 °C, respectively. Figure 4-36 shows the Mohr-Coulomb failure criteria lines of the soil under two temperatures of 8 °C and 40 °C by obtaining the maximum value of shear stress. At 8 °C, the cohesion of soil is 5.53 kPa, and the friction angle is 26.06°; at 40 °C, the cohesion of soil is 1.2 kPa, and the friction angle is 31.87°. On the surface of the piping channel that is exposed to the seepage, the normal stress can

be assumed to be zero, the shear strength is controlled by cohesion. Higher temperature resulted in lower cohesion, thus more erosion.

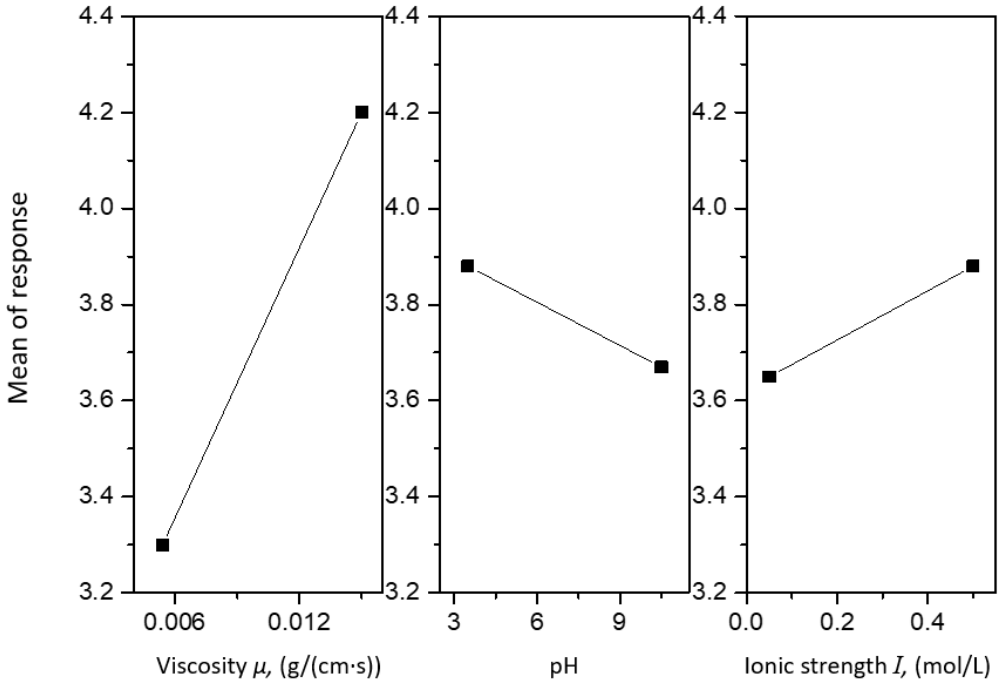

Figure 4-33. Main effects plot for response

Figure 4-33 also shows that the fluid's erosive capacity has a positive relationship with pH, i.e., higher pH causes higher erosive capacity (that is represented by lower erosion rate index); this trend is consistent with previous studies by Hubbe (1985, 1987), Sharma et al. (1992), McDowell-Boyer (1992), and Xiao et al. (2018). Further, Figure 4-33 suggests that fluid's erosive capacity has a negative relationship with ionic strength; this trend is consistent with previous studies by Sherard et al. (1972), Arulanandan et al. (1975), Reddi et al. (2000), and Xiao et al. (2018).

Figure 4-37 shows the interactive effect of each two parameters on the mean response of the erosion rate index. As for the interaction between viscosity and ionic strength, ionic strength does not affect the erosion at low viscosity ($I \approx 3.3$) since the erosion rate indexes are the same; but when the viscosity is higher (or the fluid temperature is colder), higher ionic strength causes more significant increase in erosion rate index, which means less erosion. As for the interaction between pH and ionic strength, the two lines of the low and high ionic strength are nearly parallel, which means that there is almost no interactive effect between pH and ionic strength.

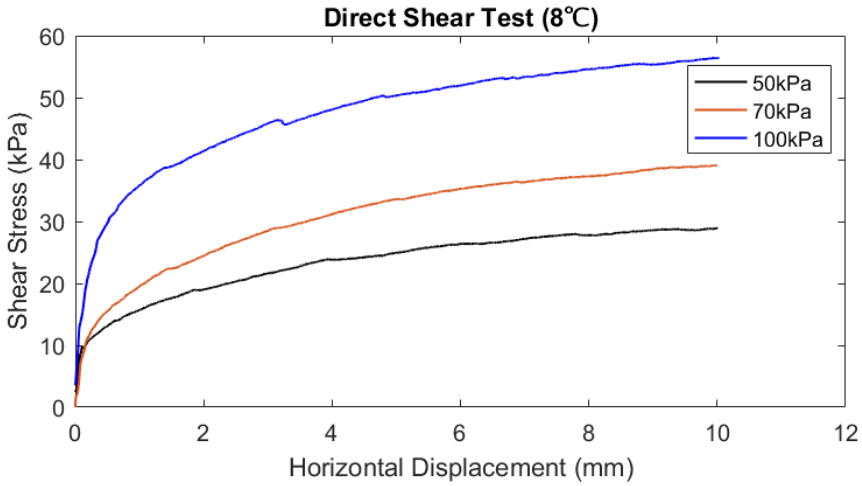

Figure 4-34. Results of the direct shear test at 8 °C

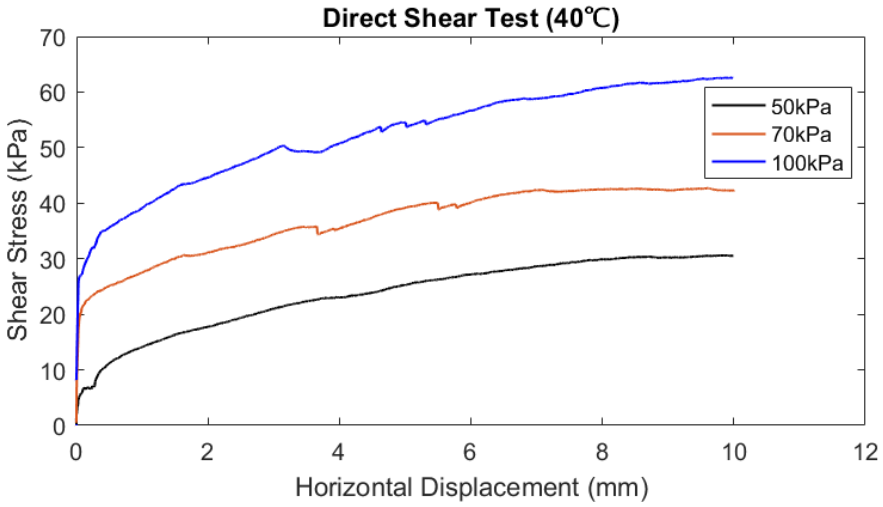

Figure 4-35. Results of the direct shear test at 40 °C

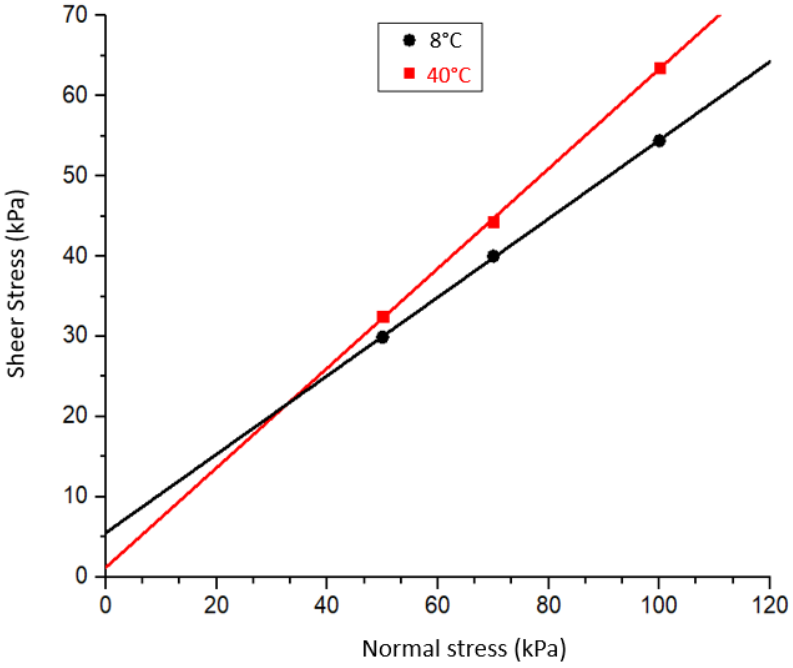

Figure 4-36. Determination of shear strength parameters using the results of direct shear tests.

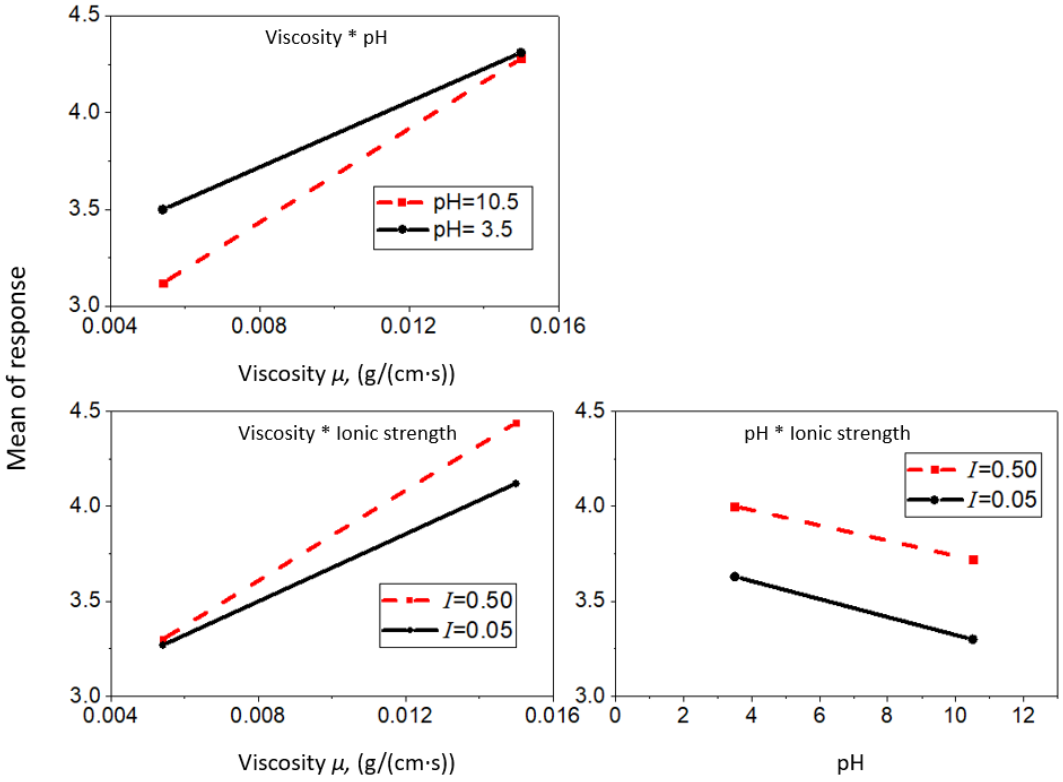

Figure 4-37. Interaction effect plot for response

CHAPTER 5 CONCLUSIONS

This research employed a statistical experimental design approach to investigate the relative and interactive effects of three physicochemical characteristics (viscosity, pH and ionic strength) of permeating fluids on piping progression of a sandy soil. An innovative experiment setup was designed and constructed to simulate the piping progression under different fluids. The erosion was characterized by the erosion rate index. ANOVA was used to analyze the relative and interactive effects of viscosity, pH and ionic strength on the sandy soil's piping progression. Temperature effect on shear strength parameters of soil was also investigated. The knowledge gained from this research is summarized as follows.

1. Viscosity, pH and ionic strength were all determined to be significant factors on the rate of erosion. The two-way interactions between viscosity and pH, and between viscosity and ionic strength were also determined to be significant interaction factors, while the interaction between pH and ionic strength did not prove to be statistically significant.
2. While the statistical experimental design and methodology may be used to study the relative and interactive effects of fluids with different physicochemical characteristics, the fluid's temperature also affected soil's strength and consequently erosion resistance. This complicated the quantitative understanding of the relative erosive capacity of the eight fluids.

3. Fluid's erosive capacity has a positive relationship with pH, i.e., higher pH causes higher erosive capacity. Fluid's erosive capacity has a negative relationship with ionic strength, i.e., higher ionic strength causes lower erosive capacity of fluid.
4. The research revealed interactive effect of each two parameters on the mean response of the erosion rate index. At low viscosity, ionic strength does not affect the erosion; but when the viscosity is higher (or the fluid temperature is colder), higher ionic strength causes much less erosion. There is almost no interactive effect between pH and ionic strength. Further research is need to provided fundamental explanations for the above phenomena.

References

Annandale, G.W. (2007). “How does water-soil interaction lead to erosion?” GSP 168, *Geotechnics of Soil Erosion, Proceedings of GeoDenver 2007*. ASCE, Reston, VA.

Arulanandan, K., Krone, R. B., and Longanathan, P. (1975). “Pore and eroding fluid influences on surface erosion on soil.” *Journal of the Geotechnical Engineering Division*, 101(1), 51–66.

Arulanandan, K. (1983). “Erosion in relation to filter design criteria in earth dams.” *Journal of Geotechnical Engineering*, 109, 682.

Arulanandan, K., Krone, R. B., & Loganathan, P. (1975). “Pore and eroding fluid influences on surface erosion on soil.” *Journal of the Geotechnical Engineering Division*, 101(1), 51-66.

ASTM-D-4221. (1999, 2005). “Standard Test Method for Dispersive Characteristics of Clay Soil by Double Hydrometer” *Annual Book of ASTM Standards, Volume 04.08, Soil and Rock (I), March 2010*.

ASTM-D-4647. (2006e1). “Standard Test Method for Identification and Classification of Dispersive Clay Soils by the Pinhole Test” *Annual Book of ASTM Standards, Volume 04.08, Soil and Rock (I)*

ASTM-D-6572. (2006). "Standard Test Methods for Determining Dispersive Characteristics of Clayey Soils by the Crumb Test" *Annual Book of ASTM Standards, Volume 04.09, Soil and Rock (II), April 2010*.

Benjamin, M. M. (2010). *Water Chemistry*. Waveland Press, Inc., Long Grove, Illinois.

Briaud, J., Chen, H., Govindasamy, A., & Storesund, R. (2008). “Levee erosion by overtopping in New Orleans during the Katrina Hurricane.” *Journal of Geotechnical and Geoenvironmental Engineering,* 134, 618.

Calvin, A. N., and Turgut, D. (1969). “Effect of temperature on strength behavior of cohesive soil.” *Highway Research Board, Special Report* 103, Conference on Effects of Temperature and Heat on Engineering Behaviour of Soils. pp. 204–219. Sponsored by the Committee on Physico-Chemical Phenomena in Soils, Washington, D.C.

Chapuis, R. P. (1986). “Quantitative measurement of the scour resistance of natural solid clays.” *Canadian Geotechnical Journal, 23*(2), 132-141.

Chapuis, R. P., & Gatien, T. (1986). “An improved rotating cylinder technique for quantitative measurements of the scour resistance of clays.” *Canadian Geotechnical Journal, 23*(1), 83-87.

Charles, J. (1997). *General Report. Special problems associated with earthfill dams*.

Emerson, W. (1964). “A classification of soil aggregates based on their coherence in water”. *Australian Journal of Soil Research, 5*(1), 47-57.

Fan, L., Nassar, R., Hwang, S., & Chou, S. (1985). “Analysis of deep bed filtration data: Modeling as a birth death process”. *AIChE Journal, 31*(11), 1781-1790.

Foster, M., Fell, R., & Spannagle, M. (2000a). The statistics of embankment dam failures and accidents. *Canadian Geotechnical Journal, 37*(5), 1000-1024.

Foster, M., Fell, R., & Spannagle, M. (2000b). A method for assessing the relative likelihood of failure of embankment dams by piping. *Canadian Geotechnical Journal, 37*(5), 1025-1061.

Hillel, D. (1998). “Fundamentals, applications, and environmental considerations.” *Environmental soil physics:* Elsevier.

Hubbe, M. A. (1985). “Detachment of colloidal hydrous oxide spheres from flat solids exposed to flow. 1: experimental system.” *Colloids and Surfaces.* (16), 227-248.

Hubbe, M. A. (1987). “Detachment of colloidal hydrous oxide spheres from flat solids exposed to flow. 3: forces of adhesion.” *Colloids and Surfaces,* (25), 311-324.

Kakuturu, S., and Reddi, L.N. (2006a). “Evaluation of the parameters influencing self-healing in earth dams.” *ASCE J. of Geotechnical and Geoenvironmental Engineering*, 132(7), 879-889.

Kakuturu, S., and Reddi, L.N. (2006b). “Mechanistic model for self-healing of core cracks in earth dams.” *ASCE J. of Geotechnical and Geoenvironmental Engineering*, 132(7), 890-901.

Kuntiwattanakul, P. (1991). “Effects of high temperature on mechanical behavior of clays.” Ph.D. thesis, Department of Civil Engineering, University of Tokyo, Tokyo, Japan.

Kandiah, A., & Arulanandan, K. (1974). “Hydraulic erosion of cohesive soils.” *Transportation Research Record 497, Transportation Research Board,* 60-68.

Kenney, T., & Lau, D. (1986). “Internal stability of granular filters: Reply.” *Canadian Geotechnical Journal, 23*(3), 420-423.

Kermani, B., Xiao, M., Stoffels, S. M., Qiu, T. (2017). “Measuring the Migration of Subgrade Fine Particles into Subbase Using Scaled Accelerated Flexible Pavement Testing – A Laboratory Study.” *International Journal of Road Material and Pavement Design,* 1-22. DOI: 10.1080/14680629.2017.1374995.

Koplik, J. (1981). “On the effective medium theory of random linear networks.” *Journal of Physics C: Solid State Physics, 14*, 4821.

Laguros, J.G. (1969). “Effect of temperature on some engineering properties of clay soils.” *Highway Research Board, Special Report* 103, Proceedings of the Conference on Effects of Temperature and Heat on Engineering Behaviour of Soils. pp. 186–193. Sponsored by the Committee on Physico-Chemical Phenomena in Soils, Washington, D.C.

McDowell-Boyer, L. M. (1992). “Chemical mobilization of micron-sized particles in saturated porous media under steady flow conditions.” *Environmental Science & Technology*, 26(3), 586–593.

Murayama, S. (1969). “Effects of temperature on elasticity of clays.” *Highway Research Board, Special Report* 103, Proceedings of the Conference on Effects of Temperature and Heat on Engineering Behaviour of Soils. pp. 194–203. Sponsored by the Committee on Physico-Chemical Phenomena in Soils, Washington, D.C.

Reddi, L., Lee, I.-M., and Bonala, M. (2000). “Comparison of internal and surface erosion using flow pump tests on a sand-kaolinite mixture.” *Geotechnical Testing Journal*, 23(1), 116-122.

Seed, R. B., Bea, R.G., Abdelmalak, R. I., Athanasopoulos-Zekkos, A., Boutwell, G.P., Bray, J.D., Cheung, C., Cobos-Roa D., Ehrensing, L., Harder Jr., L.F., Pestana, J.M., Riemer, M.F., Rogers, J.D., Storesund, R., Vera-Grunauer, X., and Wartman, J. (2008). “New Orleans and Hurricane Katrina. II: the central region and the lower Ninth Ward.” *ASCE J. of Geotechnical and Geoenvironmental Engineering*, 134(5), 718-739.

Sharma, M. M., Chamoun, H., Sita Rama Sarma, D. S. H., and Schechter, R. S. (1992). "Factors controlling the hydrodynamic detachment of particles from surfaces." *Journal of Colloid and Interface Science*, 149(1), 121–134.

Sherard, J. L., Decker, R. S., and Ryker, N. L. (1972). "Piping in earth dams of dispersive clay." Proceedings, Special Conference on Performance of Earth and Earth-supported Structures, Vol.1, Part 1, 589-626. ASCE, Reston, VA.

Sharma, M., & Yortsos, Y. (1987a). "Transport of particulate suspensions in porous media: model formulation." *AIChE Journal, 33*(10), 1636-1643.

Sharma, M., & Yortsos, Y. (1987b). "A network model for deep bed filtration processes." *AIChE Journal, 33*(10), 1644-1653.

Sharma, M., & Yortsos, Y. (1987c). "Fines migration in porous media." *AIChE Journal, 33*(10), 1654-1662.

Sherard, J. (1989). "Critical filters for impervious soils." *Journal of Geotechnical Engineering, 115*, 927.

Sherard, J., Dunnigan, L., & Talbot, J. (1984a). "Basic properties of sand and gravel filters." *Journal of Geotechnical Engineering, 110*(6), 684-700.

Sherard, J. L., Dunnigan, L. P., & Talbot, J. R. (1984b). Filters for silts and clays. *Journal of Geotechnical Engineering, 110*(6), 701-718.

Sherif, M.A., and Burrows, C.M. (1969). "Temperature effects on the unconfined shear strength of saturated cohesive soil." *Highway Research Board, Special Report* 103, Proceedings of the Conference on Effects of Temperature and Heat on Engineering Behaviour of Soils. pp. 267–272. Sponsored by the Committee on Physico-Chemical Phenomena in Soils, Washington, D.C.

Terzaghi, K., and Peck, R. B. (1948). *Soil mechanics in engineering practice*, Wiley, New York.

Toutenburg, H. (2009). *Statistical analysis of designed experiments*. Springer Science & Business Media. New York City, New York.

US Army Corps of Engineers (USACE) (2000). *Design and Construction of Levees, EM* 1110-2-1913, 30 April, 2000. Department of the Army, US Army Corps of Engineers, Washington, DC.

Visser, J. (1972). "On Hamaker constants: a comparison between Hamaker constants and Lifshitz-Van der Waals constants." *Advances in Colloid Interface Science*, 3, 331–363.

Wan, C.F., and Fell, R. (2004). "Laboratory tests on the rate of piping erosion of soils in embankment dams." *ASTM Geotechnical Testing Journal*, 27(3), 295-303.

Xiao, M., Gholizadeh-Vayghan, A., Adams, B.T., and Rajabipour, F. (2018) "Experimental investigation of the relative and interactive effects of physicochemical fluid characteristics on the incipient motion of granular particles under laminar flow conditions." *ASCE Journal of Hydraulic Engineering*. In press.

Zhang, H-L., and Han, S-J. (1996). "Viscosity and density of water + sodium chloride + potassium Chloride Solutions at 298.15 K." *Journal of Chemical Engineering Data*, 41, 516–520.

APPENDIX A: FLOW CELL DISIGN

Compaction Base Plate Design

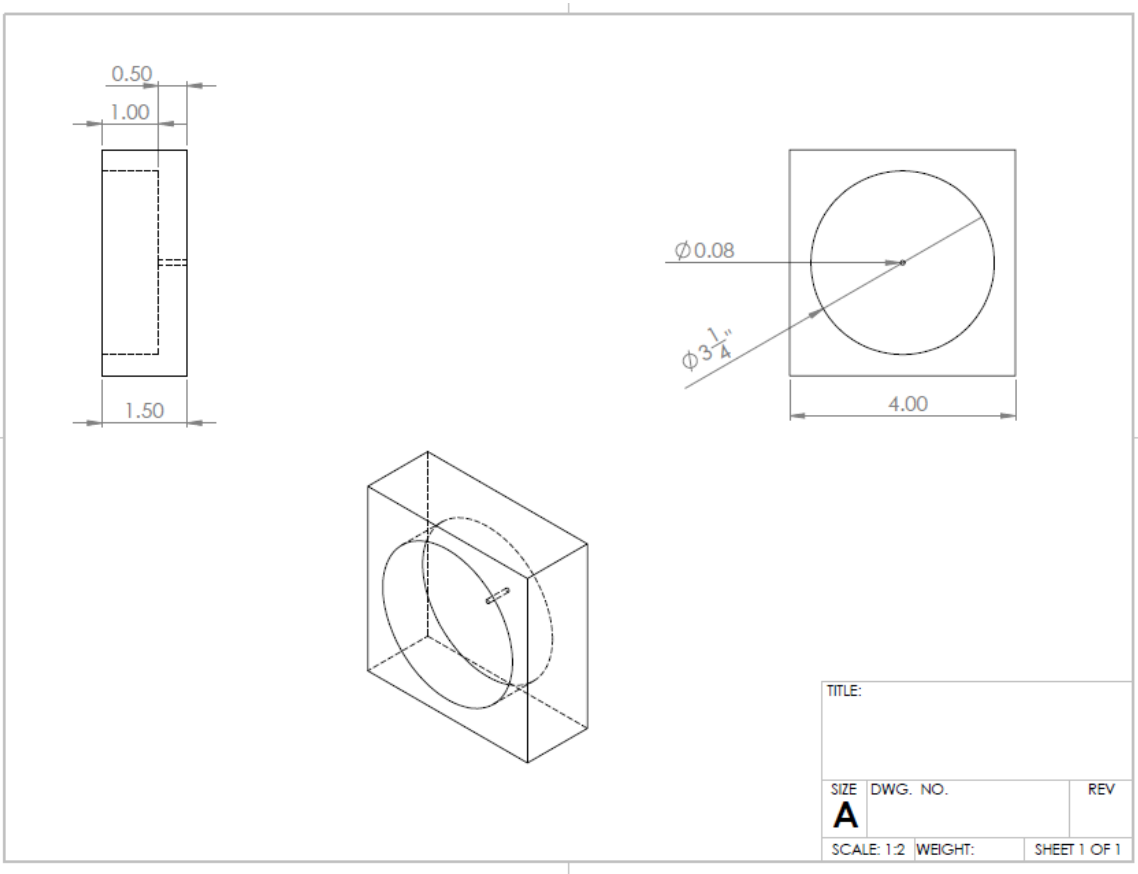

Flow Cell Design

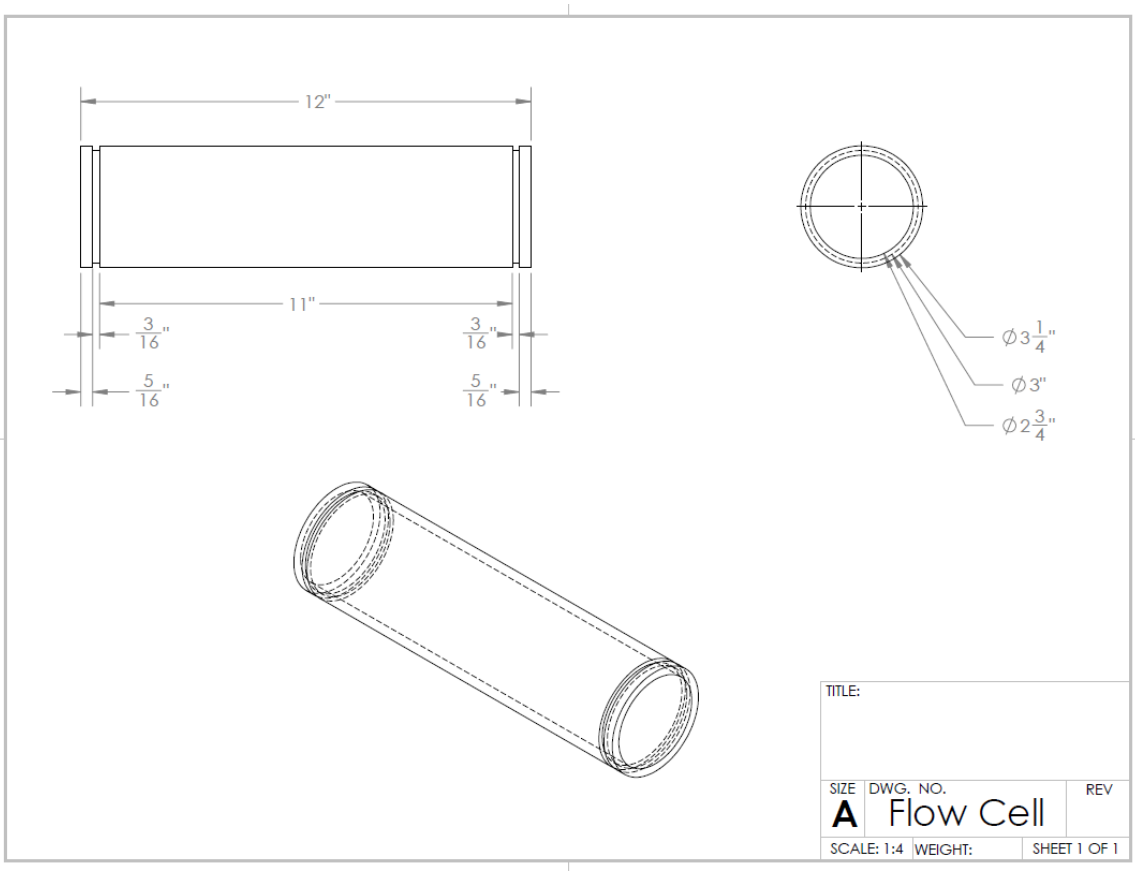

Flow Cell Assembled with Female Connection

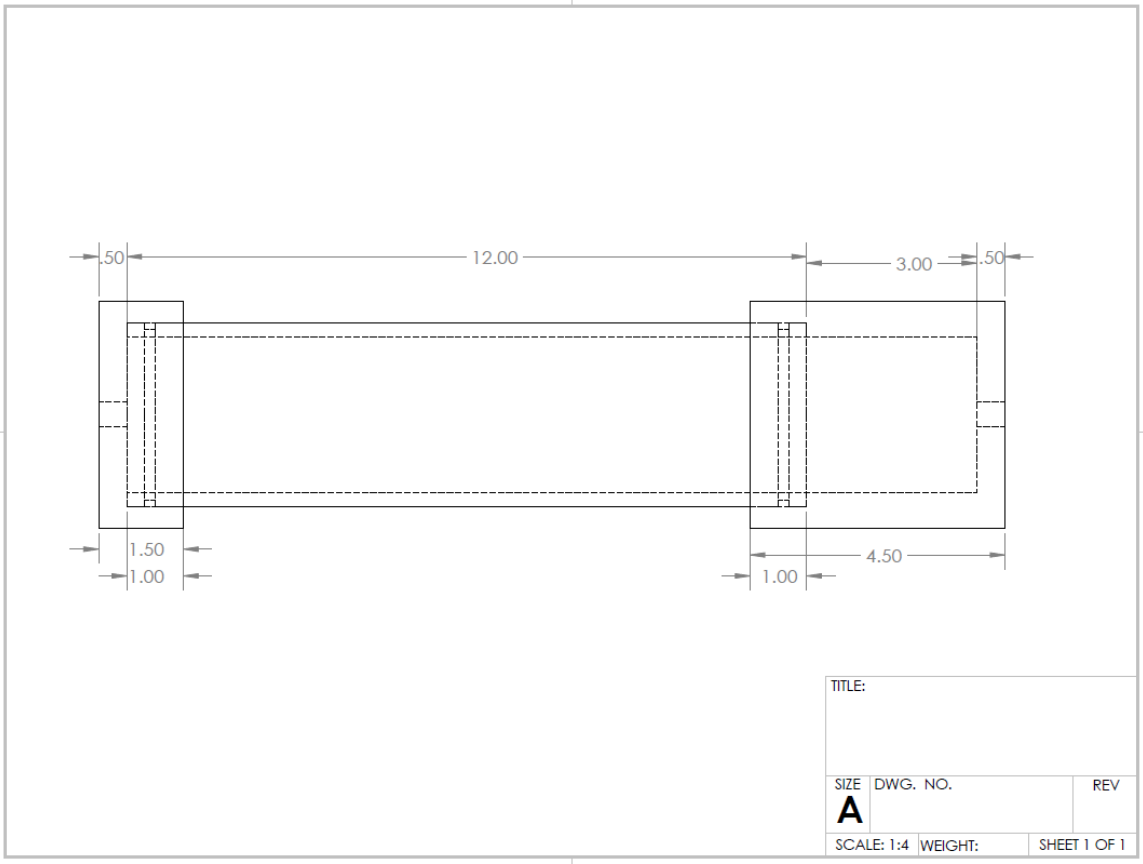

Downstream Flow Cell Cap with Female Connection

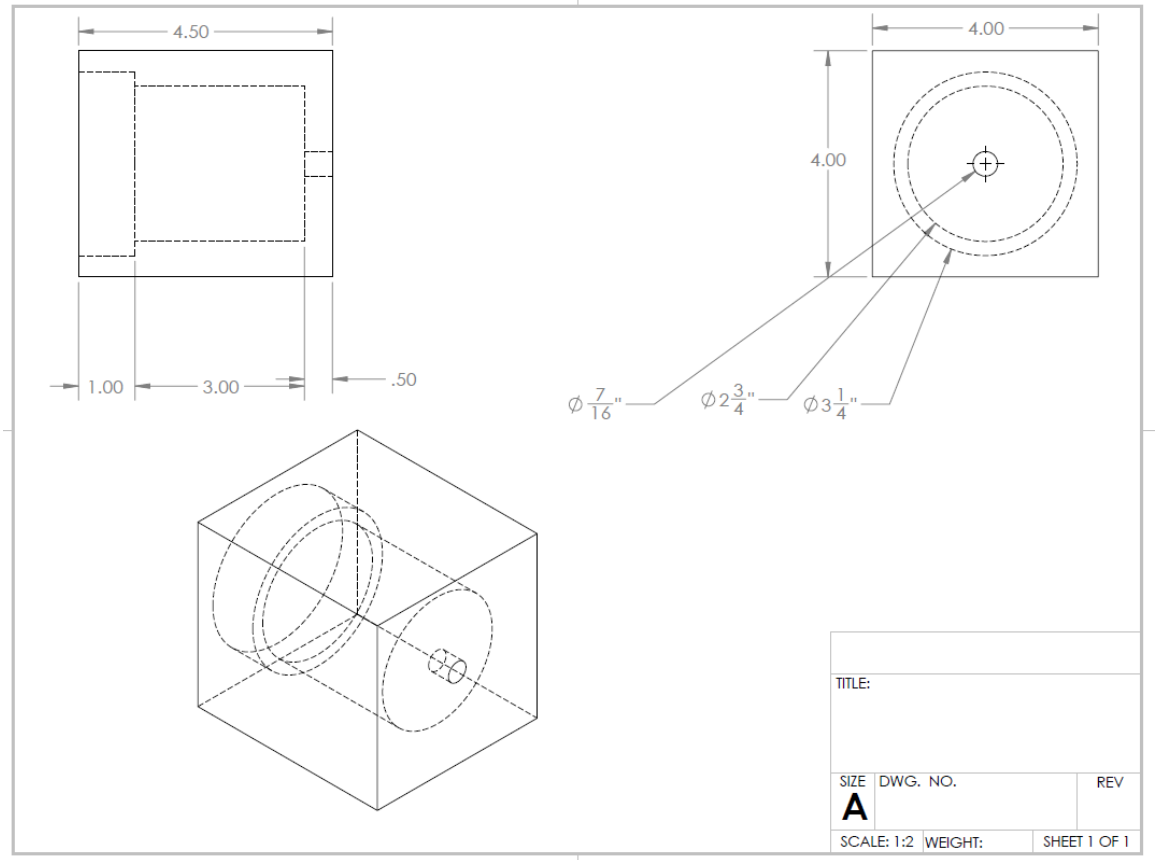

Upstream Flow Cell Cap with Female Connection

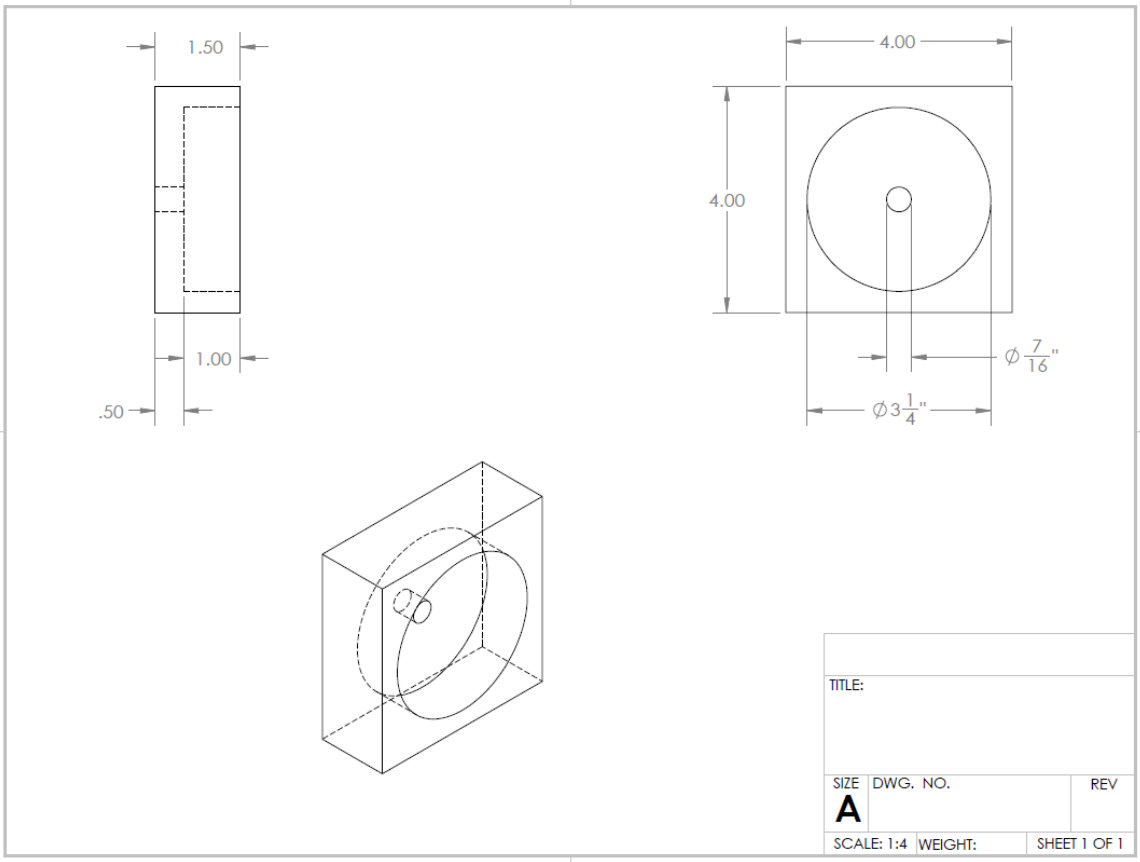

APPENDIX B: RAW DATA OF HET TEST

Fluid 1: Viscosity high, pH high, ionic strength low

Time (s)	Flow rate(m^3/s)	head difference(cm)	Hydraulic Gradient (St)
0	1.01118E-05	27.3	3.582677165
60	1.03063E-05	26.4	3.464566929
120	1.04859E-05	25.2	3.307086614
180	1.06056E-05	24	3.149606299
240	1.07103E-05	23.2	3.044619423
300	1.08151E-05	22.7	2.979002625
360	1.09348E-05	22.2	2.913385827
420	1.11144E-05	21.9	2.874015748
480	1.12041E-05	21.5	2.82152231
540	1.12939E-05	20.6	2.703412073
600	1.14735E-05	20	2.624671916
660	1.15483E-05	19.3	2.532808399
720	1.16979E-05	18.8	2.467191601
780	1.18775E-05	18.4	2.414698163
840	1.19972E-05	17.7	2.322834646
900	1.21019E-05	16.8	2.204724409
960	1.22067E-05	16.1	2.112860892
1020	1.22965E-05	15.5	2.034120735
1080	1.23713E-05	15	1.968503937
1140	1.24611E-05	14.4	1.88976378
1200	1.25359E-05	13.9	1.824146982
1260	1.25957E-05	13.7	1.797900262
1320	1.26705E-05	13.4	1.758530184
1380	1.27603E-05	12.9	1.692913386
1440	1.28351E-05	12.5	1.640419948
1500	1.288E-05	12.2	1.601049869
1560	1.291E-05	12	1.57480315
1620	1.29548E-05	11.7	1.535433071
1680	1.30147E-05	11.5	1.509186352
1740	1.30446E-05	11.4	1.496062992
1800	1.30746E-05	11.2	1.469816273
1860	1.31194E-05	11.1	1.456692913
1920	1.31643E-05	11	1.443569554
1980	1.31943E-05	10.9	1.430446194
2040	1.32092E-05	10.9	1.430446194
2100	1.32541E-05	10.8	1.417322835
2160	1.32691E-05	10.7	1.404199475
2220	1.3284E-05	10.5	1.377952756
2280	1.3299E-05	10.4	1.364829396
2340	1.3314E-05	10	1.312335958
2400	1.33289E-05	9.8	1.286089239
2460	1.33589E-05	9.7	1.272965879
2520	1.33738E-05	9.6	1.25984252

2580	1.34037E-05	9.5	1.24671916
2640	1.34187E-05	9.3	1.220472441
2700	1.34337E-05	9.2	1.207349081
2760	1.34486E-05	9.1	1.194225722
2820	1.34935E-05	9	1.181102362
2880	1.35085E-05	9	1.181102362
2940	1.35235E-05	8.9	1.167979003
3000	1.35384E-05	8.8	1.154855643
3060	1.35983E-05	8.7	1.141732283
3120	1.36282E-05	8.6	1.128608924
3180	1.36432E-05	8.6	1.128608924
3240	1.36731E-05	8.5	1.115485564
3300	1.3688E-05	8.3	1.089238845
3360	1.3703E-05	8.1	1.062992126
3420	1.3718E-05	8.1	1.062992126
3480	1.3718E-05	8	1.049868766
3540	1.3718E-05	7.9	1.036745407
3600	1.3718E-05	7.7	1.010498688
3660	1.3718E-05	7.5	0.984251969
3720	1.37329E-05	7.5	0.984251969
3780	1.37329E-05	7.4	0.971128609
3840	1.37629E-05	7.3	0.958005249
3900	1.37928E-05	7	0.918635171
3960	1.38227E-05	6.9	0.905511811
4020	1.38227E-05	6.9	0.905511811
4080	1.38377E-05	6.9	0.905511811
4140	1.38526E-05	6.9	0.905511811
4200	1.38676E-05	6.9	0.905511811
4260	1.38826E-05	6.8	0.892388451
4320	1.38826E-05	6.7	0.879265092
4380	1.38826E-05	6.7	0.879265092
4440	1.38826E-05	6.6	0.866141732
4500	1.39125E-05	6.5	0.853018373
4560	1.39125E-05	6.5	0.853018373
4620	1.39125E-05	6.5	0.853018373
4680	1.39125E-05	6.5	0.853018373
4740	1.39125E-05	6.5	0.853018373
4800	1.39125E-05	6.5	0.853018373
4860	1.39125E-05	6.4	0.839895013
4920	1.39125E-05	6.4	0.839895013
4980	1.39125E-05	6.4	0.839895013
5040	1.39424E-05	6.3	0.826771654
5100	1.39424E-05	6.3	0.826771654
5160	1.39424E-05	6.3	0.826771654
5220	1.39424E-05	6.3	0.826771654
5280	1.39424E-05	6.3	0.826771654
5340	1.39424E-05	6.3	0.826771654
5400	1.39424E-05	6.3	0.826771654

Duplicate test: Viscosity high, pH high, ionic strength low

Time (s)	Flow rate(m^3/s)	head difference(cm)	Hydraulic Gradient (St)
0	1.00071E-05	28.1	3.687664042
60	1.03512E-05	25.3	3.320209974
120	1.06355E-05	23.6	3.097112861
180	1.07552E-05	22.8	2.992125984
240	1.09498E-05	22.2	2.913385827
300	1.10545E-05	21.5	2.82152231
360	1.11293E-05	21	2.755905512
420	1.11742E-05	20.6	2.703412073
480	1.13538E-05	19.5	2.559055118
540	1.13837E-05	19.3	2.532808399
600	1.14435E-05	18.9	2.480314961
660	1.15782E-05	18	2.362204724
720	1.17727E-05	16.5	2.165354331
780	1.19523E-05	15.7	2.060367454
840	1.2057E-05	15.2	1.994750656
900	1.21618E-05	14.6	1.916010499
960	1.22366E-05	14.3	1.87664042
1020	1.22815E-05	14.2	1.86351706
1080	1.23563E-05	13.6	1.784776903
1140	1.24012E-05	13.1	1.719160105
1200	1.2476E-05	12.8	1.679790026
1260	1.25359E-05	12.4	1.627296588
1320	1.25808E-05	12.2	1.601049869
1380	1.26257E-05	11.9	1.56167979
1440	1.26855E-05	11.7	1.535433071
1500	1.27304E-05	11.6	1.522309711
1560	1.27753E-05	11.4	1.496062992
1620	1.28202E-05	11.3	1.482939633
1680	1.291E-05	11.2	1.469816273
1740	1.29698E-05	11.1	1.456692913
1800	1.29997E-05	11.1	1.456692913
1860	1.30446E-05	11	1.443569554
1920	1.31045E-05	10.9	1.430446194
1980	1.31643E-05	10.7	1.404199475
2040	1.31943E-05	10.6	1.391076115
2100	1.32092E-05	10.2	1.338582677
2160	1.32391E-05	10	1.312335958
2220	1.32691E-05	9.9	1.299212598
2280	1.3299E-05	9.8	1.286089239
2340	1.33738E-05	9.7	1.272965879
2400	1.34037E-05	9.5	1.24671916
2460	1.34187E-05	9.4	1.233595801
2520	1.34486E-05	9.3	1.220472441
2580	1.34935E-05	9.2	1.207349081

2640	1.35235E-05	9.2	1.207349081
2700	1.35384E-05	9.1	1.194225722
2760	1.35534E-05	9	1.181102362
2820	1.36132E-05	8.9	1.167979003
2880	1.36282E-05	8.8	1.154855643
2940	1.36282E-05	8.8	1.154855643
3000	1.36581E-05	8.7	1.141732283
3060	1.36581E-05	8.5	1.115485564
3120	1.36581E-05	8.3	1.089238845
3180	1.3703E-05	8.3	1.089238845
3240	1.37479E-05	8.2	1.076115486
3300	1.37778E-05	8.1	1.062992126
3360	1.37928E-05	7.9	1.036745407
3420	1.37928E-05	7.7	1.010498688
3480	1.38078E-05	7.7	1.010498688
3540	1.38078E-05	7.6	0.997375328
3600	1.38377E-05	7.5	0.984251969
3660	1.38526E-05	7.2	0.94488189
3720	1.38526E-05	7.1	0.93175853
3780	1.38826E-05	7.1	0.93175853
3840	1.38826E-05	7.1	0.93175853
3900	1.38975E-05	7.1	0.93175853
3960	1.39125E-05	7.1	0.93175853
4020	1.39275E-05	7	0.918635171
4080	1.39275E-05	6.9	0.905511811
4140	1.39424E-05	6.9	0.905511811
4200	1.39424E-05	6.8	0.892388451
4260	1.39574E-05	6.7	0.879265092
4320	1.39574E-05	6.7	0.879265092
4380	1.39574E-05	6.7	0.879265092
4440	1.39574E-05	6.7	0.879265092
4500	1.39724E-05	6.7	0.879265092
4560	1.39724E-05	6.7	0.879265092
4620	1.39724E-05	6.6	0.866141732
4680	1.39873E-05	6.6	0.866141732
4740	1.39873E-05	6.6	0.866141732
4800	1.40023E-05	6.5	0.853018373
4860	1.40023E-05	6.5	0.853018373
4920	1.40023E-05	6.5	0.853018373
4980	1.40023E-05	6.5	0.853018373
5040	1.40172E-05	6.4	0.839895013
5100	1.40172E-05	6.4	0.839895013
5160	1.40172E-05	6.4	0.839895013
5220	1.40322E-05	6.4	0.839895013
5280	1.40322E-05	6.4	0.839895013
5340	1.40322E-05	6.4	0.839895013
5400	1.40322E-05	6.4	0.839895013

Fluid 2: Viscosity high, pH high, ionic strength high

Time (s)	Flow rate(m^3/s)	head difference(cm)	Hydraulic Gradient (St)
0	9.18409E-06	30	3.937007874
60	9.36365E-06	28.5	3.74015748
120	9.51328E-06	27.7	3.635170604
180	9.57313E-06	27.1	3.556430446
240	9.60306E-06	26.8	3.517060367
300	9.63299E-06	26.5	3.477690289
360	9.72277E-06	25.9	3.398950131
420	9.75269E-06	25.6	3.359580052
480	9.82751E-06	25	3.280839895
540	9.82751E-06	25	3.280839895
600	9.82751E-06	25	3.280839895
660	9.84247E-06	24.8	3.254593176
720	9.84247E-06	24.8	3.254593176
780	9.84247E-06	24.8	3.254593176
840	9.84247E-06	24.8	3.254593176
900	9.85744E-06	24.7	3.241469816
960	9.85744E-06	24.7	3.241469816
1020	9.85744E-06	24.7	3.241469816
1080	9.85744E-06	24.7	3.241469816
1140	9.85744E-06	24.7	3.241469816
1200	9.85744E-06	24.7	3.241469816
1260	9.8724E-06	24.6	3.228346457
1320	9.8724E-06	24.6	3.228346457
1380	9.8724E-06	24.6	3.228346457
1440	9.8724E-06	24.6	3.228346457
1500	9.8724E-06	24.6	3.228346457
1560	9.8724E-06	24.6	3.228346457
1620	9.8724E-06	24.6	3.228346457
1680	9.8724E-06	24.6	3.228346457
1740	9.8724E-06	24.6	3.228346457
1800	9.8724E-06	24.6	3.228346457
1860	9.8724E-06	24.6	3.228346457
1920	9.8724E-06	24.6	3.228346457
1980	9.8724E-06	24.6	3.228346457
2040	9.8724E-06	24.6	3.228346457
2100	9.8724E-06	24.6	3.228346457
2160	9.8724E-06	24.6	3.228346457
2220	9.8724E-06	24.6	3.228346457
2280	9.8724E-06	24.6	3.228346457
2340	9.8724E-06	24.6	3.228346457
2400	9.8724E-06	24.6	3.228346457
2460	9.8724E-06	24.6	3.228346457
2520	9.8724E-06	24.6	3.228346457
2580	9.8724E-06	24.6	3.228346457
2640	9.8724E-06	24.6	3.228346457

2700	9.8724E-06	24.6	3.228346457
2760	9.8724E-06	24.6	3.228346457
2820	9.8724E-06	24.6	3.228346457
2880	9.8724E-06	24.6	3.228346457
2940	9.8724E-06	24.6	3.228346457
3000	9.8724E-06	24.6	3.228346457
3060	9.8724E-06	24.6	3.228346457
3120	9.8724E-06	24.6	3.228346457
3180	9.8724E-06	24.6	3.228346457
3240	9.8724E-06	24.6	3.228346457
3300	9.8724E-06	24.6	3.228346457
3360	9.8724E-06	24.6	3.228346457
3420	9.8724E-06	24.6	3.228346457
3480	9.8724E-06	24.6	3.228346457
3540	9.8724E-06	24.6	3.228346457
3600	9.8724E-06	24.6	3.228346457
3660	9.8724E-06	24.6	3.228346457
3720	9.8724E-06	24.6	3.228346457
3780	9.8724E-06	24.6	3.228346457
3840	9.8724E-06	24.6	3.228346457
3900	9.8724E-06	24.6	3.228346457
3960	9.8724E-06	24.6	3.228346457
4020	9.8724E-06	24.6	3.228346457
4080	9.8724E-06	24.6	3.228346457
4140	9.8724E-06	24.6	3.228346457
4200	9.8724E-06	24.6	3.228346457
4260	9.8724E-06	24.6	3.228346457
4320	9.8724E-06	24.6	3.228346457
4380	9.8724E-06	24.6	3.228346457
4440	9.8724E-06	24.6	3.228346457
4500	9.8724E-06	24.6	3.228346457
4560	9.8724E-06	24.6	3.228346457
4620	9.8724E-06	24.6	3.228346457
4680	9.8724E-06	24.6	3.228346457
4740	9.8724E-06	24.6	3.228346457
4800	9.8724E-06	24.6	3.228346457
4860	9.8724E-06	24.6	3.228346457
4920	9.8724E-06	24.6	3.228346457
4980	9.8724E-06	24.6	3.228346457
5040	9.8724E-06	24.6	3.228346457
5100	9.8724E-06	24.6	3.228346457
5160	9.8724E-06	24.6	3.228346457
5220	9.8724E-06	24.6	3.228346457
5280	9.8724E-06	24.6	3.228346457
5340	9.8724E-06	24.6	3.228346457
5400	9.8724E-06	24.6	3.228346457

Duplicate test: Viscosity high, pH high, ionic strength high

Time (s)	Flow rate(m^3/s)	head difference(cm)	Hydraulic Gradient (St)
0	9.11E-06	30.1	3.950131
60	9.27E-06	28.8	3.779528
120	9.44E-06	27.8	3.648294
180	9.53E-06	27.1	3.55643
240	9.6E-06	26.5	3.47769
300	9.65E-06	26.1	3.425197
360	9.68E-06	25.8	3.385827
420	9.68E-06	25.8	3.385827
480	9.68E-06	25.8	3.385827
540	9.69E-06	25.5	3.346457
600	9.69E-06	25.5	3.346457
660	9.69E-06	25.5	3.346457
720	9.69E-06	25.5	3.346457
780	9.71E-06	25.3	3.32021
840	9.71E-06	25.3	3.32021
900	9.71E-06	25.3	3.32021
960	9.71E-06	25.3	3.32021
1020	9.71E-06	25.3	3.32021
1080	9.72E-06	25.2	3.307087
1140	9.72E-06	25.2	3.307087
1200	9.72E-06	25.2	3.307087
1260	9.72E-06	25.2	3.307087
1320	9.74E-06	25.1	3.293963
1380	9.74E-06	25.1	3.293963
1440	9.74E-06	25.1	3.293963
1500	9.75E-06	25	3.28084
1560	9.75E-06	25	3.28084
1620	9.75E-06	25	3.28084
1680	9.75E-06	25	3.28084
1740	9.75E-06	25	3.28084
1800	9.75E-06	25	3.28084
1860	9.75E-06	25	3.28084
1920	9.75E-06	25	3.28084
1980	9.75E-06	25	3.28084
2040	9.77E-06	24.9	3.267717
2100	9.77E-06	24.9	3.267717
2160	9.77E-06	24.9	3.267717
2220	9.77E-06	24.9	3.267717
2280	9.77E-06	24.9	3.267717
2340	9.77E-06	24.9	3.267717
2400	9.77E-06	24.9	3.267717
2460	9.77E-06	24.9	3.267717
2520	9.77E-06	24.9	3.267717
2580	9.77E-06	24.9	3.267717
2640	9.77E-06	24.9	3.267717

2700	9.77E-06	24.9	3.267717
2760	9.77E-06	24.9	3.267717
2820	9.77E-06	24.9	3.267717
2880	9.77E-06	24.9	3.267717
2940	9.77E-06	24.9	3.267717
3000	9.77E-06	24.9	3.267717
3060	9.77E-06	24.9	3.267717
3120	9.77E-06	24.9	3.267717
3180	9.77E-06	24.9	3.267717
3240	9.77E-06	24.9	3.267717
3300	9.77E-06	24.9	3.267717
3360	9.77E-06	24.9	3.267717
3420	9.77E-06	24.9	3.267717
3480	9.77E-06	24.9	3.267717
3540	9.77E-06	24.9	3.267717
3600	9.77E-06	24.9	3.267717
3660	9.77E-06	24.9	3.267717
3720	9.77E-06	24.9	3.267717
3780	9.77E-06	24.9	3.267717
3840	9.77E-06	24.9	3.267717
3900	9.77E-06	24.9	3.267717
3960	9.77E-06	24.9	3.267717
4020	9.77E-06	24.9	3.267717
4080	9.77E-06	24.9	3.267717
4140	9.77E-06	24.9	3.267717
4200	9.77E-06	24.9	3.267717
4260	9.77E-06	24.9	3.267717
4320	9.77E-06	24.9	3.267717
4380	9.77E-06	24.9	3.267717
4440	9.77E-06	24.9	3.267717
4500	9.77E-06	24.9	3.267717
4560	9.77E-06	24.9	3.267717
4620	9.77E-06	24.9	3.267717
4680	9.77E-06	24.9	3.267717
4740	9.77E-06	24.9	3.267717
4800	9.77E-06	24.9	3.267717
4860	9.77E-06	24.9	3.267717
4920	9.77E-06	24.9	3.267717
4980	9.77E-06	24.9	3.267717
5040	9.77E-06	24.9	3.267717
5100	9.77E-06	24.9	3.267717
5160	9.77E-06	24.9	3.267717
5220	9.77E-06	24.9	3.267717
5280	9.77E-06	24.9	3.267717
5340	9.77E-06	24.9	3.267717
5400	9.77E-06	24.9	3.267717

Fluid 3: Viscosity high, pH low, ionic strength low

Time (s)	Flow rate(m^3/s)	head difference(cm)	Hydraulic Gradient (St)
0	1.02E-05	26.7	3.503937
60	1.04E-05	25.8	3.385827
120	1.06E-05	24.8	3.254593
180	1.07E-05	24.2	3.175853
240	1.08E-05	23.8	3.12336
300	1.1E-05	23	3.018373
360	1.11E-05	22.5	2.952756
420	1.11E-05	22	2.887139
480	1.12E-05	21.7	2.847769
540	1.13E-05	21.3	2.795276
600	1.15E-05	20.4	2.677165
660	1.16E-05	19.8	2.598425
720	1.17E-05	19.1	2.506562
780	1.18E-05	18.6	2.440945
840	1.19E-05	18.2	2.388451
900	1.2E-05	17.5	2.296588
960	1.22E-05	16.6	2.178478
1020	1.23E-05	15.9	2.086614
1080	1.24E-05	15.3	2.007874
1140	1.25E-05	14.8	1.942257
1200	1.26E-05	14.2	1.863517
1260	1.27E-05	13.7	1.7979
1320	1.27E-05	13.5	1.771654
1380	1.28E-05	13.2	1.732283
1440	1.29E-05	12.7	1.666667
1500	1.29E-05	12.3	1.614173
1560	1.3E-05	12	1.574803
1620	1.3E-05	11.8	1.548556
1680	1.31E-05	11.5	1.509186
1740	1.31E-05	11.3	1.48294
1800	1.31E-05	11.2	1.469816
1860	1.32E-05	11	1.44357
1920	1.32E-05	10.9	1.430446
1980	1.32E-05	10.8	1.417323
2040	1.32E-05	10.7	1.404199
2100	1.32E-05	10.7	1.404199
2160	1.33E-05	10.6	1.391076
2220	1.33E-05	10.5	1.377953
2280	1.33E-05	10.3	1.351706
2340	1.33E-05	10.2	1.338583
2400	1.34E-05	9.8	1.286089
2460	1.34E-05	9.6	1.259843
2520	1.35E-05	9.5	1.246719
2580	1.35E-05	9.4	1.233596

2640	1.35E-05	9.3	1.220472
2700	1.35E-05	9.1	1.194226
2760	1.35E-05	9	1.181102
2820	1.36E-05	8.9	1.167979
2880	1.36E-05	8.8	1.154856
2940	1.36E-05	8.8	1.154856
3000	1.36E-05	8.7	1.141732
3060	1.36E-05	8.6	1.128609
3120	1.36E-05	8.5	1.115486
3180	1.37E-05	8.4	1.102362
3240	1.37E-05	8.4	1.102362
3300	1.37E-05	8.3	1.089239
3360	1.37E-05	8.1	1.062992
3420	1.37E-05	7.9	1.036745
3480	1.37E-05	7.9	1.036745
3540	1.37E-05	7.8	1.023622
3600	1.38E-05	7.7	1.010499
3660	1.38E-05	7.5	0.984252
3720	1.38E-05	7.3	0.958005
3780	1.38E-05	7.3	0.958005
3840	1.38E-05	7.2	0.944882
3900	1.39E-05	7.1	0.931759
3960	1.39E-05	6.8	0.892388
4020	1.39E-05	6.7	0.879265
4080	1.39E-05	6.7	0.879265
4140	1.39E-05	6.7	0.879265
4200	1.39E-05	6.7	0.879265
4260	1.39E-05	6.7	0.879265
4320	1.39E-05	6.6	0.866142
4380	1.39E-05	6.5	0.853018
4440	1.39E-05	6.5	0.853018
4500	1.4E-05	6.4	0.839895
4560	1.4E-05	6.3	0.826772
4620	1.4E-05	6.3	0.826772
4680	1.4E-05	6.3	0.826772
4740	1.4E-05	6.3	0.826772
4800	1.4E-05	6.3	0.826772
4860	1.4E-05	6.3	0.826772
4920	1.4E-05	6.2	0.813648
4980	1.4E-05	6.2	0.813648
5040	1.4E-05	6.2	0.813648
5100	1.4E-05	6.1	0.800525
5160	1.4E-05	6.1	0.800525
5220	1.4E-05	6.1	0.800525
5280	1.4E-05	6.1	0.800525
5340	1.4E-05	6.1	0.800525
5400	1.4E-05	6.1	0.800525

Duplicate test: Viscosity high, pH low, ionic strength low

Time (s)	Flow rate(m^3/s)	head difference(cm)	Hydraulic Gradient (St)
0	1.04E-05	27.6	3.622047
60	1.05E-05	26.7	3.503937
120	1.07E-05	25.7	3.372703
180	1.08E-05	25.1	3.293963
240	1.09E-05	24.7	3.24147
300	1.1E-05	23.9	3.136483
360	1.11E-05	23.4	3.070866
420	1.12E-05	22.9	3.005249
480	1.12E-05	22.6	2.965879
540	1.13E-05	22.2	2.913386
600	1.14E-05	21.3	2.795276
660	1.17E-05	20.7	2.716535
720	1.17E-05	20	2.624672
780	1.18E-05	19.5	2.559055
840	1.19E-05	19.1	2.506562
900	1.2E-05	18.2	2.388451
960	1.22E-05	17.3	2.270341
1020	1.24E-05	16.3	2.139108
1080	1.25E-05	15.7	2.060367
1140	1.26E-05	15.2	1.994751
1200	1.26E-05	14.6	1.91601
1260	1.27E-05	14.3	1.87664
1320	1.27E-05	14.2	1.863517
1380	1.28E-05	13.6	1.784777
1440	1.29E-05	13.1	1.71916
1500	1.29E-05	12.8	1.67979
1560	1.3E-05	12.4	1.627297
1620	1.31E-05	12.2	1.60105
1680	1.32E-05	11.9	1.56168
1740	1.32E-05	11.7	1.535433
1800	1.33E-05	11.6	1.52231
1860	1.33E-05	11.4	1.496063
1920	1.33E-05	11.3	1.48294
1980	1.34E-05	11.2	1.469816
2040	1.34E-05	11.1	1.456693
2100	1.34E-05	11.1	1.456693
2160	1.34E-05	11	1.44357
2220	1.34E-05	10.9	1.430446
2280	1.34E-05	10.7	1.404199
2340	1.35E-05	10.6	1.391076
2400	1.35E-05	10.2	1.338583
2460	1.36E-05	10	1.312336
2520	1.36E-05	9.9	1.299213
2580	1.36E-05	9.8	1.286089
2640	1.37E-05	9.7	1.272966

2700	1.37E-05	9.5	1.246719
2760	1.37E-05	9.4	1.233596
2820	1.37E-05	9.3	1.220472
2880	1.37E-05	9.2	1.207349
2940	1.38E-05	9.2	1.207349
3000	1.38E-05	9.1	1.194226
3060	1.38E-05	9	1.181102
3120	1.38E-05	8.9	1.167979
3180	1.38E-05	8.8	1.154856
3240	1.39E-05	8.8	1.154856
3300	1.39E-05	8.7	1.141732
3360	1.39E-05	8.5	1.115486
3420	1.39E-05	8.3	1.089239
3480	1.39E-05	8.3	1.089239
3540	1.39E-05	8.2	1.076115
3600	1.4E-05	8.1	1.062992
3660	1.4E-05	7.9	1.036745
3720	1.4E-05	7.7	1.010499
3780	1.4E-05	7.7	1.010499
3840	1.4E-05	7.6	0.997375
3900	1.4E-05	7.5	0.984252
3960	1.4E-05	7.2	0.944882
4020	1.4E-05	7.1	0.931759
4080	1.4E-05	7.1	0.931759
4140	1.41E-05	7.1	0.931759
4200	1.41E-05	7.1	0.931759
4260	1.41E-05	7.1	0.931759
4320	1.41E-05	7	0.918635
4380	1.41E-05	6.9	0.905512
4440	1.41E-05	6.9	0.905512
4500	1.41E-05	6.8	0.892388
4560	1.41E-05	6.7	0.879265
4620	1.41E-05	6.7	0.879265
4680	1.41E-05	6.7	0.879265
4740	1.41E-05	6.7	0.879265
4800	1.41E-05	6.7	0.879265
4860	1.41E-05	6.7	0.879265
4920	1.41E-05	6.6	0.866142
4980	1.42E-05	6.6	0.866142
5040	1.42E-05	6.6	0.866142
5100	1.42E-05	6.5	0.853018
5160	1.42E-05	6.5	0.853018
5220	1.42E-05	6.5	0.853018
5280	1.42E-05	6.5	0.853018
5340	1.42E-05	6.5	0.853018
5400	1.42E-05	6.5	0.853018

Fluid 4: Viscosity high, pH low, ionic strength high

Time (s)	Flow rate(m^3/s)	head difference(cm)	Hydraulic Gradient (St)
0	9.41E-06	30.7	4.028871
60	9.59E-06	29.4	3.858268
120	9.74E-06	28.9	3.792651
180	9.78E-06	28.6	3.753281
240	9.89E-06	28.2	3.700787
300	9.92E-06	27.9	3.661417
360	1E-05	27.3	3.582677
420	1.01E-05	26.8	3.51706
480	1.01E-05	26.8	3.51706
540	1.01E-05	26.8	3.51706
600	1.01E-05	26.8	3.51706
660	1.01E-05	26.8	3.51706
720	1.01E-05	26.7	3.503937
780	1.01E-05	26.7	3.503937
840	1.01E-05	26.7	3.503937
900	1.01E-05	26.7	3.503937
960	1.01E-05	26.6	3.490814
1020	1.01E-05	26.6	3.490814
1080	1.01E-05	26.6	3.490814
1140	1.01E-05	26.6	3.490814
1200	1.01E-05	26.6	3.490814
1260	1.01E-05	26.5	3.47769
1320	1.01E-05	26.5	3.47769
1380	1.01E-05	26.5	3.47769
1440	1.01E-05	26.5	3.47769
1500	1.01E-05	26.5	3.47769
1560	1.01E-05	26.5	3.47769
1620	1.01E-05	26.5	3.47769
1680	1.01E-05	26.4	3.464567
1740	1.01E-05	26.4	3.464567
1800	1.01E-05	26.4	3.464567
1860	1.01E-05	26.4	3.464567
1920	1.01E-05	26.4	3.464567
1980	1.01E-05	26.4	3.464567
2040	1.02E-05	26.3	3.451444
2100	1.02E-05	26.3	3.451444
2160	1.02E-05	26.3	3.451444
2220	1.02E-05	26.3	3.451444
2280	1.02E-05	26.3	3.451444
2340	1.02E-05	26.3	3.451444
2400	1.02E-05	26.3	3.451444
2460	1.02E-05	26.3	3.451444
2520	1.02E-05	26.3	3.451444
2580	1.02E-05	26.3	3.451444
2640	1.02E-05	26.3	3.451444

2700	1.02E-05	26.3	3.451444
2760	1.02E-05	26.3	3.451444
2820	1.02E-05	26.3	3.451444
2880	1.02E-05	26.3	3.451444
2940	1.02E-05	26.3	3.451444
3000	1.02E-05	26.3	3.451444
3060	1.02E-05	26.3	3.451444
3120	1.02E-05	26.3	3.451444
3180	1.02E-05	26.3	3.451444
3240	1.02E-05	26.3	3.451444
3300	1.02E-05	26.3	3.451444
3360	1.02E-05	26.3	3.451444
3420	1.02E-05	26.3	3.451444
3480	1.02E-05	26.3	3.451444
3540	1.02E-05	26.3	3.451444
3600	1.02E-05	26.3	3.451444
3660	1.02E-05	26.3	3.451444
3720	1.02E-05	26.3	3.451444
3780	1.02E-05	26.3	3.451444
3840	1.02E-05	26.3	3.451444
3900	1.02E-05	26.3	3.451444
3960	1.02E-05	26.3	3.451444
4020	1.02E-05	26.3	3.451444
4080	1.02E-05	26.3	3.451444
4140	1.02E-05	26.3	3.451444
4200	1.02E-05	26.3	3.451444
4260	1.02E-05	26.3	3.451444
4320	1.02E-05	26.3	3.451444
4380	1.02E-05	26.3	3.451444
4440	1.02E-05	26.3	3.451444
4500	1.02E-05	26.3	3.451444
4560	1.02E-05	26.3	3.451444
4620	1.02E-05	26.3	3.451444
4680	1.02E-05	26.3	3.451444
4740	1.02E-05	26.3	3.451444
4800	1.02E-05	26.3	3.451444
4860	1.02E-05	26.3	3.451444
4920	1.02E-05	26.3	3.451444
4980	1.02E-05	26.3	3.451444
5040	1.02E-05	26.3	3.451444
5100	1.02E-05	26.3	3.451444
5160	1.02E-05	26.3	3.451444
5220	1.02E-05	26.3	3.451444
5280	1.02E-05	26.3	3.451444
5340	1.02E-05	26.3	3.451444
5400	1.02E-05	26.3	3.451444

Duplicate test: Viscosity high, pH low, ionic strength high

Time (s)	Flow rate(m^3/s)	head difference(cm)	Hydraulic Gradient (St)
0	9.48E-06	30.3	3.976378
60	9.66E-06	29.1	3.818898
120	9.81E-06	28.3	3.713911
180	9.86E-06	28	3.674541
240	9.92E-06	27.6	3.622047
300	9.95E-06	27.4	3.595801
360	1E-05	27.1	3.55643
420	1.01E-05	26.9	3.530184
480	1.01E-05	26.8	3.51706
540	1.01E-05	26.5	3.47769
600	1.01E-05	26.5	3.47769
660	1.01E-05	26.5	3.47769
720	1.01E-05	26.4	3.464567
780	1.01E-05	26.4	3.464567
840	1.01E-05	26.4	3.464567
900	1.01E-05	26.4	3.464567
960	1.02E-05	26.3	3.451444
1020	1.02E-05	26.3	3.451444
1080	1.02E-05	26.3	3.451444
1140	1.02E-05	26.3	3.451444
1200	1.02E-05	26.3	3.451444
1260	1.02E-05	26.2	3.43832
1320	1.02E-05	26.2	3.43832
1380	1.02E-05	26.2	3.43832
1440	1.02E-05	26.2	3.43832
1500	1.02E-05	26.2	3.43832
1560	1.02E-05	26.2	3.43832
1620	1.02E-05	26.2	3.43832
1680	1.02E-05	26.2	3.43832
1740	1.02E-05	26.2	3.43832
1800	1.02E-05	26.2	3.43832
1860	1.02E-05	26.2	3.43832
1920	1.02E-05	26.2	3.43832
1980	1.02E-05	26.2	3.43832
2040	1.02E-05	26.2	3.43832
2100	1.02E-05	26.2	3.43832
2160	1.02E-05	26.2	3.43832
2220	1.02E-05	26.2	3.43832
2280	1.02E-05	26.2	3.43832
2340	1.02E-05	26.2	3.43832
2400	1.02E-05	26.2	3.43832
2460	1.02E-05	26.2	3.43832
2520	1.02E-05	26.2	3.43832
2580	1.02E-05	26.2	3.43832

2640	1.02E-05	26.2	3.43832
2700	1.02E-05	26.2	3.43832
2760	1.02E-05	26.2	3.43832
2820	1.02E-05	26.2	3.43832
2880	1.02E-05	26.2	3.43832
2940	1.02E-05	26.2	3.43832
3000	1.02E-05	26.2	3.43832
3060	1.02E-05	26.2	3.43832
3120	1.02E-05	26.2	3.43832
3180	1.02E-05	26.2	3.43832
3240	1.02E-05	26.2	3.43832
3300	1.02E-05	26.2	3.43832
3360	1.02E-05	26.2	3.43832
3420	1.02E-05	26.2	3.43832
3480	1.02E-05	26.2	3.43832
3540	1.03E-05	26.1	3.425197
3600	1.03E-05	26.1	3.425197
3660	1.03E-05	26.1	3.425197
3720	1.03E-05	26.1	3.425197
3780	1.03E-05	26.1	3.425197
3840	1.03E-05	26.1	3.425197
3900	1.03E-05	26.1	3.425197
3960	1.03E-05	26.1	3.425197
4020	1.03E-05	26.1	3.425197
4080	1.03E-05	26.1	3.425197
4140	1.03E-05	26.1	3.425197
4200	1.03E-05	26.1	3.425197
4260	1.03E-05	26.1	3.425197
4320	1.03E-05	26.1	3.425197
4380	1.03E-05	26.1	3.425197
4440	1.03E-05	26.1	3.425197
4500	1.03E-05	26.1	3.425197
4560	1.03E-05	26.1	3.425197
4620	1.03E-05	26.1	3.425197
4680	1.03E-05	26.1	3.425197
4740	1.03E-05	26.1	3.425197
4800	1.03E-05	26.1	3.425197
4860	1.03E-05	26.1	3.425197
4920	1.03E-05	26.1	3.425197
4980	1.03E-05	26.1	3.425197
5040	1.03E-05	26.1	3.425197
5100	1.03E-05	26.1	3.425197
5160	1.03E-05	26.1	3.425197
5220	1.03E-05	26.1	3.425197
5280	1.03E-05	26.1	3.425197
5340	1.03E-05	26.1	3.425197
5400	1.03E-05	26.1	3.425197

Fluid 5: Viscosity low, pH low, ionic strength high

Time (s)	Flow rate(m^3/s)	head difference(cm)	Hydraulic Gradient (St)
0	1.08E-05	28.5	3.740157
60	1.14E-05	24.7	3.24147
120	1.21E-05	21.5	2.821522
180	1.24E-05	20.2	2.650919
240	1.26E-05	17.1	2.244094
300	1.31E-05	14.5	1.902887
360	1.33E-05	13.4	1.75853
420	1.34E-05	12.8	1.67979
480	1.35E-05	12.5	1.64042
540	1.36E-05	12.3	1.614173
600	1.36E-05	12.2	1.60105
660	1.36E-05	12	1.574803
720	1.37E-05	11.7	1.535433
780	1.37E-05	11.7	1.535433
840	1.37E-05	11.5	1.509186
900	1.37E-05	11.4	1.496063
960	1.37E-05	11.4	1.496063
1020	1.37E-05	11.2	1.469816
1080	1.37E-05	11.2	1.469816
1140	1.37E-05	11.2	1.469816
1200	1.37E-05	11.2	1.469816

Duplicate test: Viscosity low, pH low, ionic strength high

Time (s)	Flow rate(m^3/s)	head difference(cm)	Hydraulic Gradient (St)
0	1.08E-05	28	3.674541
60	1.15E-05	23.7	3.110236
120	1.22E-05	19.3	2.532808
180	1.27E-05	17.8	2.335958
240	1.3E-05	15.5	2.034121
300	1.32E-05	14.3	1.87664
360	1.33E-05	13.7	1.7979
420	1.34E-05	13.4	1.75853
480	1.35E-05	13	1.706037
540	1.36E-05	12.6	1.653543
600	1.37E-05	12.2	1.60105
660	1.37E-05	11.8	1.548556
720	1.38E-05	11.5	1.509186
780	1.38E-05	11.2	1.469816
840	1.38E-05	11	1.44357
900	1.39E-05	10.9	1.430446
960	1.39E-05	10.9	1.430446
1020	1.39E-05	10.9	1.430446
1080	1.39E-05	10.8	1.417323
1140	1.39E-05	10.8	1.417323
1200	1.39E-05	10.8	1.417323

Fluid 6: Viscosity low, pH low, ionic strength low

Time (s)	Flow rate(m^3/s)	head difference(cm)	Hydraulic Gradient (St)
0	1.11E-05	25.7	3.372703
60	1.18E-05	20.5	2.690289
120	1.24E-05	16.4	2.152231
180	1.27E-05	15.1	1.981627
240	1.3E-05	13.5	1.771654
300	1.36E-05	12.7	1.666667
360	1.38E-05	12.3	1.614173
420	1.39E-05	11.9	1.56168
480	1.39E-05	11.7	1.535433
540	1.4E-05	11.4	1.496063
600	1.41E-05	11.2	1.469816
660	1.42E-05	11	1.44357
720	1.42E-05	10.9	1.430446
780	1.42E-05	10.8	1.417323
840	1.42E-05	10.7	1.404199
900	1.42E-05	10.7	1.404199
960	1.43E-05	10.6	1.391076
1020	1.43E-05	10.6	1.391076
1080	1.43E-05	10.6	1.391076
1140	1.43E-05	10.6	1.391076
1200	1.43E-05	10.6	1.391076

Duplicate test: Viscosity low, pH low, ionic strength low

Time (s)	Flow rate(m^3/s)	head difference(cm)	Hydraulic Gradient (St)
0	1.12E-05	25.9	3.39895
60	1.19E-05	21	2.755906
120	1.25E-05	16.7	2.191601
180	1.28E-05	16	2.099738
240	1.31E-05	14.8	1.942257
300	1.37E-05	13	1.706037
360	1.38E-05	12.6	1.653543
420	1.39E-05	12.3	1.614173
480	1.4E-05	11.9	1.56168
540	1.41E-05	11.6	1.52231
600	1.41E-05	11.3	1.48294
660	1.42E-05	10.9	1.430446
720	1.42E-05	10.8	1.417323
780	1.42E-05	10.7	1.404199
840	1.43E-05	10.6	1.391076
900	1.43E-05	10.5	1.377953
960	1.43E-05	10.3	1.351706
1020	1.43E-05	10.3	1.351706
1080	1.43E-05	10.3	1.351706
1140	1.43E-05	10.3	1.351706
1200	1.43E-05	10.3	1.351706
1260	1.43E-05	10.3	1.351706
1320	1.43E-05	10.3	1.351706

Fluid 7: Viscosity low, pH high, ionic strength high

Time (s)	Flow rate(m^3/s)	head difference(cm)	Hydraulic Gradient (St)
0	1.03E-05	30	3.937008
30	1.32E-05	14.7	1.929134
60	1.37E-05	10.6	1.391076
90	1.43E-05	7	0.918635
120	1.45E-05	5.6	0.734908
150	1.45E-05	5.4	0.708661
180	1.47E-05	4	0.524934
210	1.48E-05	3.8	0.498688
240	1.48E-05	3.6	0.472441
270	1.48E-05	3.4	0.446194
300	1.48E-05	3.2	0.419948
330	1.48E-05	2.9	0.380577
360	1.49E-05	2.8	0.367454
390	1.49E-05	2.7	0.354331
420	1.49E-05	2.5	0.328084
450	1.5E-05	2.3	0.301837
480	1.5E-05	2.2	0.288714
510	1.5E-05	2.1	0.275591
540	1.51E-05	2	0.262467
570	1.51E-05	2	0.262467
600	1.51E-05	2	0.262467

Duplicate test: Viscosity low, pH high, ionic strength high

Time (s)	Flow rate(m^3/s)	head difference(cm)	Hydraulic Gradient (St)
0	1.03E-05	30	3.937008
30	1.3E-05	14.4	1.889764
60	1.37E-05	10.9	1.430446
90	1.45E-05	7.1	0.931759
120	1.46E-05	5.8	0.761155
150	1.48E-05	5.1	0.669291
180	1.49E-05	4.2	0.551181
210	1.49E-05	4	0.524934
240	1.49E-05	3.6	0.472441
270	1.5E-05	3.3	0.433071
300	1.5E-05	3.1	0.406824
330	1.5E-05	3	0.393701
360	1.5E-05	2.9	0.380577
390	1.51E-05	2.6	0.341207
420	1.51E-05	2.5	0.328084
450	1.51E-05	2.3	0.301837
480	1.51E-05	2.1	0.275591
510	1.51E-05	1.9	0.249344
540	1.51E-05	1.7	0.223097
570	1.51E-05	1.7	0.223097
600	1.51E-05	1.7	0.223097

Fluid 8: Viscosity low, pH high, ionic strength low

Time (s)	Flow rate(m^3/s)	head difference(cm)	Hydraulic Gradient (St)
0	1.06E-05	29.5	3.871391
30	1.27E-05	18.6	2.440945
60	1.39E-05	10.4	1.364829
90	1.46E-05	6.5	0.853018
120	1.48E-05	5.1	0.669291
150	1.5E-05	4	0.524934
180	1.51E-05	3.5	0.459318
210	1.51E-05	3.2	0.419948
240	1.52E-05	3	0.393701
270	1.52E-05	2.6	0.341207
300	1.52E-05	2.5	0.328084
330	1.52E-05	2.3	0.301837
360	1.53E-05	2	0.262467
390	1.53E-05	2	0.262467
420	1.53E-05	1.8	0.23622
450	1.53E-05	1.8	0.23622
480	1.53E-05	1.6	0.209974
510	1.53E-05	1.4	0.183727
540	1.53E-05	1.2	0.15748
570	1.54E-05	0.9	0.11811
600	1.54E-05	0.9	0.11811

Duplicate test: Viscosity low, pH high, ionic strength low

Time (s)	Flow rate(m^3/s)	head difference(cm)	Hydraulic Gradient (St)
0	1.05E-05	31	4.068241
30	1.26E-05	19	2.493438
60	1.37E-05	10.9	1.430446
90	1.45E-05	6.9	0.905512
120	1.47E-05	5	0.656168
150	1.49E-05	4.2	0.551181
180	1.5E-05	3.7	0.485564
210	1.51E-05	3.4	0.446194
240	1.51E-05	3.1	0.406824
270	1.51E-05	2.8	0.367454
300	1.52E-05	2.7	0.354331
330	1.52E-05	2.5	0.328084
360	1.52E-05	2.4	0.314961
390	1.52E-05	2.2	0.288714
420	1.53E-05	2	0.262467
450	1.53E-05	2	0.262467
480	1.53E-05	1.7	0.223097
510	1.53E-05	1.5	0.19685
540	1.53E-05	1.2	0.15748
570	1.53E-05	1.2	0.15748
600	1.53E-05	1.2	0.15748